DRL No. 73/DRD NO. SE-7

DOE/JPL-955055-78/1

Distribution Category UC-63

Silicon Solar Cell Process Development, Fabrication and Analysis

SECOND QUARTERLY REPORT

For Period Covering

January thru March, 1979

Prepared by

Joseph A. Minahan

Approved by

Jack A. Castle

JPL Contract No. 955055

Spectrolab, Inc.

12500 Gladstone Avenue

Sylmar, California 91342

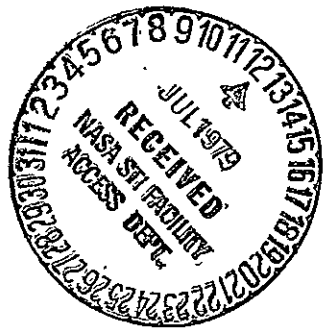

"The JPL Low-Cost Silicon Solar Array Project is sponsored by the U.S. Department of Energy and forms part of the Solar Photovoltaic Conversion Program to initiate a major effort toward the development of low-cost solar arrays. This work was performed for the Jet Propulsion Laboratory, California Institute of Technology by agreement between NASA and DOE."

DRL No. 73/DRD NO. SE-7

DOE/JPL-955055-78/1

Distribution Category UC-63

Silicon Solar Cell Process Development, Fabrication and Analysis

SECOND QUARTERLY REPORT

For Period Covering

January thru March, 1979

Prepared by

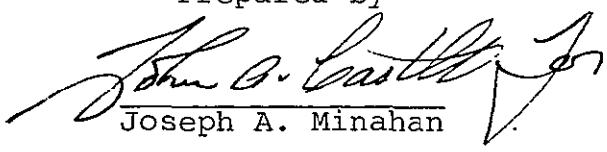

Joseph A. Minahan

Approved by

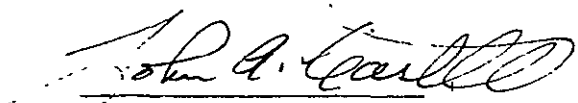

Jack A. Castle

JPL Contract No. 955055

Spectrolab, Inc.

12500 Gladstone Avenue

Sylmar, California 91342

"The JPL Low-Cost Silicon Solar Array Project is sponsored by the U.S. Department of Energy and forms part of the Solar Photovoltaic Conversion Program to initiate a major effort toward the development of low-cost solar arrays. This work was performed for the Jet Propulsion Laboratory, California Institute of Technology by agreement between NASA and DOE."

ABSTRACT

Solar cells have been constructed from polycrystalline silicon sheet material (10 cm x 10 cm Wacker Silso). These cells have been made using conventional aerospace methods and serve as the so-called "baseline cell" for analysis and comparison with cells to be made from similar material, but using optimized processing techniques.

Before and during the processing of the Wacker baseline cells in a cleaned diffusion tube, control cells were built using the baseline method.

All cells were measured on the Spectrolab Mark III Solar Simulator at air mass zero and 28°C. Average efficiency for the Wacker Silso baseline cells, using the total device area, was 9.5%. Efficiency was found to vary with location in the sheet. Center regions had higher efficiencies, 9.9% average, whereas corner and edge regions had lower efficiencies, 8.9% average. In general, the efficiency falls off with distance from the center of the sheet. This could possibly be a result of radial grain growth at the edges and grain growth along the axial direction in the core region of the casting.

Control cells made from aerospace grade silicon using the baseline process had average efficiency of 11.7%. Like the polycrystalline cells, the control cells had antireflection coatings of tantalum pentoxide.

Table of Contents

List of Tables

List of Figures

I. Introduction

The goal of this contract is to evaluate the solar cell potential of unconventional silicon sheets of interest to the Large Area Silicon Sheet Task of the Low Cost Solar Array Project. This includes not only the processing of the material into a statistically significant number of solar cells by conventional methods, but also by what might be considered an optimal method suited for each particular material. In this report we consider the baseline process, the characterization of cells made by this process from Wacker Silso polycrystalline sheet and an analysis of the results. Finally, we conclude from this analysis what steps might be used to optimize the processing of such material into solar cells.

Measurements, both direct and derived, for this study include current-voltage at AMO and 28^{o}C, dark current-voltage, spectral response, curve fill factor, efficiency, maximum power, short circuit current, and open circuit voltage.

II. Technical Discussion

A number of diverse silicon materials will be made into solar cells by both conventional and optimized processing methods during the period of this contract. In order to assure a reasonable amount of reproducibility within each material group of cells a specific control program was proposed. It was believed that this program would minimize the occurrence of wafer contamination sometimes encountered in such work. Some processing steps are apparently more susceptible to error than others and their effect upon the results can be both subtle and difficult to trace. Because elevated temperatures are used and since contamination usually takes place via a thermal pathway considerable emphasis has been given to reducing the possibility of contamination arising during the diffusion process.

2.1 Control Program

Quartz diffusion tubes were purchased and dedicated to the program. After cleaning a diffusion tube the procedure is as follows: A control lot consisting of eight 2 x 2 cm^2 1-3 ohm-cm silicon wafers is processed into cells and measured. If the results are satisfactory the tube is then used to process the unconventional material into cells. If the results are not satisfactory the tube is again cleaned and eight more control wafers are processed into cells. Only after satisfactory cells have been processed from the control wafers is the cleaned diffusion tube considered suitable for baseline or optimized cell processing. When the tube has been proven satisfactory, as described above, the sheet material is processed along with control wafers. On the diffusion boat, control wafers are placed at the front and back of the boat and are spaced between the sheet wafers such that every one of the latter is within the immediate locale of a control wafer. The control wafers are then processed along with the sheet wafers and used both for comparison with the sheet cells and as processing monitors. Whenever the process is changed or when the material is changed the tube is cleaned and the above steps taken before any further processing of sheet cells is pursued in that diffusion tube.

It has been suggested that such a methodology leads to better reproducibility within a sheet lot and from run to run. It is obvious that other steps in the process can also lead to unsatisfactory cells and these must be monitored by the processor with an equal degree of concern.

2.2 Process Outline

The sheet material is supplied by JPL. The control wafers, 1-3 ohm-cm, p type, are produced in Spectrolab's crystal growing facility. The Wacker Silso 10 cm x 10 cm x .04 cm sheets are chem-polished to a thickness of about .23 mm and then cut into 2 cm by 2 cm wafers by means of a Tempress dicing saw.

After cleaning to remove both organic and metallic impurities, that might be present, the wafers are loaded onto a quartz boat and placed within a 2" diameter quartz diffusion tube maintained at 850^{o}C by a Thermco furnace. The diffusion schedule is arranged such that the wafers are loaded and placed in the furnace within an hour of the wafer cleaning. During the furnace period a three step gas sequence is maintained. For the first five minutes following boat insertion a pure nitrogen gas flow is maintained. For the next ten minutes a gas flow mixture of oxygen and phosphine is used. This is the deposition step and should result in a surface concentration of greater than 10^{20} cm^{-3} of phosphorus. The third and final part of the sequence is a twenty minute period of nitrogen-only in the tube. This is known as the drive and should result in a Gaussian distribution of the dopant. The boat is then removed from the furnace at a slow rate, cooled and the wafers taken from the boat for further processing.

Following diffusion the wafers are briefly placed in an HF solution to remove any oxides resulting from the thermal process. Sheet rho is then measured to estimate junction depth.

In the next step the wafers are masked and back-etched to remove the junction from the back of the wafers. Then the wafers are cleaned and placed in an evaporator where titanium, palladium and silver are deposited through metal masks onto the back and front of the wafers. The wafers are sintered in an inert atmosphere to minimize contact resistance and increase adherence. After this they are ready for the deposition of an antireflecting tantalum pentoxide film.

The final step in the processing is the edge etch, where the wafers are etched to remove any extraneous metal deposits that could lead to a shunting of the cell.

Electrical measurements are then made of the finished cells. An I-V curve is plotted for each cell at air mass zero and 28°C on the Spectrolab Mark III Solar Simulator. From the I-V curve the short circuit current, the current and voltage at maximum power, the open circuit voltage, the curve fill factor, maximum power, and conversion efficiency are determined. The latter is based upon total device area.

The spectral sensitivity at thirteen different wavelengths is measured for each cell as well as dark forward and reverse currents. Following tabulation and analysis of data the completed cells are delivered to JPL for their testing procedures.

2.3 Results

A complete tabulation of I-V data is given in Tables 1 through 4. The Wacker run is identified by W-, followed by a number. Each of the run numbers follows a chronological sequence. Unsatisfactory control runs are not reported here since they were not followed by a run of sheet material, but nonetheless they have been identified in the sequence. Although not all the unsatisfactory control runs could be attributed to a contaminated tube the latter was assumed and the tube was cleaned and another control group processed.

Run W-4 consisted of wafers cut from sheet centers, i.e. the four 2 cm x 2 cm wafers that could be cut from a single sheet. Of the six wafers (from two Wacker sheets) that were started in the processing sequence one broke during the V/I probe and another broke in the cleanup following edge etch. Conversion efficiency given for each individual cell is based upon total device area.

Run W-11 consisted of a composite made up from two Wacker Silso sheets and included wafers cut from corners, edges and center

Table 1

Solar Cell Data

Run W-4

Conditions: AMO; 28°C; calculated for total device area of 4 cm^2 and irradiance of 135.3 $mWcm^{-2}$; AR coated (Ta_2O_5).

S/N	ρ_s	I_M, a	V_M, V	I_{sc}, a	V_{oc}, V	CFF	η, %	P_{max}
* 1	57.1	.132	.500	.142	.594	.78	12.0	66.2
* 2	55.3	.133	.505	.142	.598	.79	12.5	67.3
* 5	57.6	.130	.500	.139	.594	.79	12.0	65.0
* 6	53.9	.132	.503	.142	.598	.78	12.3	66.6
* 9	54.2	.133	.505	.141	.598	.80	12.5	67.3
*10	52.6	.133	.505	.143	.598	.78	12.4	67.0
*13	49.6	.129	.497	.142	.596	.76	11.8	63.9
*14	51.0	.131	.507	.141	.598	.79	12.3	66.4
Aver.	53.9	.132	.503	.142	.597	.78	12.2	66.2
S	2.8	.002	.003	.001	.002	.01	.3	1.2
3	56.9	.124	.450	.133	.549	.76	10.3	55.8
4	58.0	.126	.455	.134	.554	.77	10.6	57.3
11	52.8	.124	.453	.133	.557	.76	10.4	56.2
12	51.4	.122	.459	.132	.557	.76	10.3	56.0
8	54.2	broken						
7	-	broken						
Aver.	54.7	.124	.454	.133	.554	.76	10.4	56.3
S	2.8	.002	.004	.001	.004	.005	.14	.67
Range,Cont	8.0	.004	.006	.004	.004	.04	.7	3.4
Range,Poly	6.6	.004	.009	.002	.008	.01	.3	1.5

* Control cell

(cont'd)

Table 1
(Continued)

Where;

ρ_s = sheet rho, ohms per square

I_M = current at maximum power, amperes

V_M = voltage at maximum power, volts

I_{sc} = short circuit current, amperes

V_{oc} = open circuit voltage

CFF = curve fill factor

η = conversion efficiency at maximum power, percent

P_{max} = maximum power, milliwatts

S = sample standard deviation

Table 2

Run W-11

Conditions: See Table 1

S/N	ρ_s	I_M, a	V_m, V	I_{sc}, a	V_{oc}, V	CFF	η, %	P_{max}
1	59	.1186	.442	.1304	.544	.74	9.7	52
2	63	.1214	.449	.1325	.547	.75	10.1	55
3	59	.106	.445	.1334	.549	.64	8.7	47
4	63	.1188	.442	.1296	.546	.74	9.7	53
5	63	.1176	.442	.1294	.542	.74	9.6	52
6	59	.1204	.441	.1312	.549	.74	9.8	53
7	59	.1222	.445	.1316	.546	.76	10.0	54
8	59	.1196	.447	.1319	.546	.74	9.9	53
9	54	.1204	.445	.1326	.549	.74	9.9	54
13	54	.1232	.442	.1342	.550	.74	10.1	54
14	54	.1210	.448	.1328	.548	.74	10.0	54
15	54	.1192	.438	.1295	.544	.74	9.6	52
16	54	.1176	.432	.1269	.537	.75	9.4	51
17	54	.1220	.452	.1320	.554	.75	10.2	55
18	54	.1176	.441	.1283	.544	.74	9.6	52
21	54	.1158	.441	.1275	.541	.74	9.4	51
22	54	.1208	.436	.1302	.543	.74	9.7	53
23	54	.1188	.446	.1297	.545	.75	9.8	53
24	54	.1190	.443	.1293	.542	.75	9.7	53
25	54	.1176	.438	.1290	.541	.74	9.5	52
26	54	.1196	.442	.1304	.547	.74	9.8	53
27	54	.1176	.443	.1280	.545	.75	9.6	52
28	54	.1190	.440	.1299	.550	.73	9.7	52
Aver.	56	.1189	.443	.1304	.546	.74	9.7	53
S	3.4	.0033	.004	.0019	.005	.02	.31	1.6
Range	9	.0162	.02	.0073	.017	.12	1.5	8

Table 2
(Continued)

	S/N	ρ_s	I_M, a	V_M, V	I_{sc}, a	V_{oc}, V	CFF	η, %	P_{max}
	* 1	54	.1302	.491	.1413	.599	.76	11.8	64
	* 3	54	.1230	.495	.1365	.597	.75	11.3	61
	* 4	50	.1258	.501	.1398	.598	.75	11.6	63
	* 5	54	.1276	.504	.1391	.601	.77	11.9	64
	* 6	50	.1246	.493	.1389	.594	.74	11.4	61
	* 7	48	.1240	.500	.1383	.597	.75	11.5	62
	* 8	43	.1274	.498	.1399	.597	.76	11.7	63
Aver		50	.1261	.497	.1391	.598	.75	11.6	63
S		4.1	.0025	.005	.0015	.002	.02	.22	1.3
Range		11	.0072	.013	.0048	.004	.03	.6	3

* Control cell

Table 3

Run W-12

Conditions: See Table 1

	S/N	ρ_s	I_M, a	V_M, V	I_{sc}, a	V_{oc}, V	CFF	η, %	P_{max}
Corner	A-1	40.8	.1090	.443	.1185	.543	.75	8.9	48
Corner	D-1	45.3	.1094	.448	.1201	.543	.75	9.1	49
Center	D-2	40.8	.1116	.442	.1216	.543	.75	9.1	49
Center	D-3	45.3	.1116	.442	.1242	.542	.73	9.1	49
Center	D-4	45.3	.1160	.458	.1262	.554	.76	9.8	53
Center	D-5	45.3	.1148	.452	.1299	.551	.73	9.6	52
Center	D-6	40.8	.1198	.451	.1291	.554	.76	10.0	54
Center	D-7	45.3	.1148	.448	.1242	.548	.76	9.5	51
Center	D-8	45.3	.1148	.455	.1259	.554	.76	9.7	52
Center	D-9	45.3	.1098	.449	.1221	.549	.74	9.1	49
Edge	D-10	40.8	.1160	.448	.1259	.547	.75	9.6	52
Edge	D-11	45.3	.1096	.438	.1197	.543	.74	8.9	48
Edge	D-12	40.8	.1118	.448	.1226	.546	.75	9.3	50
Edge	D-13	40.8	.1004	.437	.1212	.540	.67	8.1	44
Edge	D-14	40.8	.1080	.442	.1207	.544	.73	8.8	48
Edge	D-15	40.8	.1090	.438	.1202	.541	.73	8.8	48
Ave poly		43.1	.1117	.446	.1233	.546	.74	9.2	50
S		2.3	.0045	.006	.0034	.005	.02	.48	2.5
Ave Edge		42.5	.1100	.444	.1223	.546	.73	9.0	49
Ave Center		44.2	.1164	.452	.1274	.552	.75	9.7	53
Ave Corner		43.1	.1104	.444	.1211	.543	.75	9.1	49
	* 1	36.3	.1182	.500	.1291	.598	.77	10.9	59
	* 2	31.7	.1256	.501	.1384	.601	.76	11.6	63
	* 4	40.8	.1162	.495	.1293	.595	.75	10.6	58
	* 5	36.3	.1218	.500	.1312	.601	.77	11.3	61
	* 8	40.8	.1252	.500	.1352	.599	.77	11.6	63
Ave		36.9	.1214	.499	.1326	.599	.76	11.2	61

* Control cell

Table 4

Run W-13

Conditions: See Table 1

S/N	ρ_s	I_M, a	V_M, V	I_{sc}, a	V_{oc}, V	CFF	η, %	P_{max}	
1	54.4	.104	.431	.114	.539	.73	9.0	45	(3.7 cm^2)
4	49.9	.104	.432	.114	.538	.73	9.0	45	(3.7 cm^2)
6	45.3	.112	.424	.126	.541	.70	8.8	47	
7	49.9	.118	.451	.130	.553	.74	9.8	53	
8	49.9	.117	.452	.127	.552	.75	9.8	53	
11	49.9	.113	.432	.124	.542	.73	9.0	49	
12	49.9	.121	.448	.132	.553	.74	10.0	54	
13	45.3	.121	.448	.131	.554	.75	10.0	54	
14	49.9	.120	.445	.130	.548	.75	9.9	53	
16	49.9	.110	.431	.120	.535	.74	9.0	47	(3.9 cm^2)
17	45.3	.116	.438	.125	.546	.74	9.4	51	
18	49.9	.122	.445	.131	.549	.75	10.0	54	
19	45.3	.118	.439	.129	.544	.74	9.6	52	
21	45.3	.108	.425	.118	.529	.74	8.5	46	
22	49.9	.113	.430	.125	.538	.72	9.0	46	
24	45.3	.113	.432	.122	.536	.75	9.0	49	
25	45.3	.093	.427	.103	.531	.73	7.6	40	(3.8 cm^2)
Ave	48.3	.114	.438	.125	.544	.74	9.3	49.6	
S	2.8	.006	.009	.006	.008	.01	.62	3.4	
Range	9.1	.029	.027	.029	.025	.05	1.7	9	
*1	45.3	.132	.489	.137	.594	.79	11.9	65	
*2	45	.104	.484	.137	.588	.62	9.3	50	
*3	45	.123	.495	.139	.595	.74	11.3	61	
*4	45	.120	.489	.139	.593	.71	10.8	59	
*5	41	.2w4	.489	.137	.596	.74	11.2	61	
*6	45	.122	.502	.133	.596	.77	11.4	61	
*7	41	.123	.500	.136	.598	.76	11.4	62	
*8	45	.124	.493	.139	.597	.74	11.3	61	
Ave	44	.122	.493	.137	.595	.73	11.1	60	
S	1.9	.008	.006	.002	.003	.05	.8	4.4	
Range	4	.028	.018	.006	.010	.17	2.6	15	

* Control cell

NOTE: See Figure 1, page 9, for cell's position in sheet

regions. No attempt has been made to identify locations on the wafer and as such these results are representative of the total sheet. Three sheet wafer cells and one control cell were damaged during processing. One of the sheet cells was broken during the unloading operation following contact evaporation while the remainder were broken during the inking and bake operation just prior to the edge etch step.

Run W-12 was made up of wafers from a single sheet of Wacker Silso with the exception of one wafer. This exception was a corner wafer and replaced a corner wafer damaged during the cutting operation. Of the sixteen sheet wafers none were damaged during processing whereas two controls were broken during back etch and one control wafer was broken while unloading after contact evaporation.

Run W-13 consisted of wafers cut from a single sheet. In this instance wafers were cut from the sheet such that they included the very edge. Twenty-five wafers were cut and one wafer was lost during this operation. Two were broken during the back etch masking step, two were found to be undersized and unsuitable for the evaporation holder, three were broken during edge etch and one was undersized, hence disqualified. If one divides the sheet into three regions of outer edge wafers, interior wafers and center wafer one discerns the radial pattern of reduced efficiency as one proceeds from the center of the sheet to the outer border.

In the outer edge of wafers the average efficiency is 8.7%, in the interior region of wafers the average efficiency is 9.8% while the conversion efficiency of the center wafer is 10.0%. This and other parameters are plotted in Figure 1 as a function of position on the Wacker sheet.

1	2	3	4	5
9.0%			9.0%	
6	7	8	9	10
8.8%	9.8%	9.8%		
11	12	13	14	15
9.0%	10.0%	10.0%	9.9%	
16	17	18	19	20
9.0%	9.4%	10.0%	9.6%	
21	22	23	24	25
8.5%	9.0%		9.0%	7.6%

Zone 1 $\bar{\eta}$ = 8.7%, $\bar{V}_{oc}$ = .539V, $\bar{I}_{sc}$ = .1203

Zone 2 $\bar{\eta}$ = 9.8 $\bar{V}_{oc}$ = .549 $\bar{I}_{sc}$ = .1291

Zone 3 $\bar{\eta}$ = 10.0 $\bar{V}_{oc}$ = .554 $\bar{I}_{sc}$ = .1310

Fig. 2. Wafer order and conversion efficiency of Wacker Silso Sheer for Run W-13. Outside edge is Zone 1, inner region is Zone 2 and the center wafer is Zone 3.

2.3.1 Current-Voltage

A number of I-V curves are presented in Figures 2 through 12. These are typical of the Wacker and control cells produced by the baseline process. Two curves from run W-13 are shown in Figures 11 and 12. The first of these is for a cell cut from the center of a Wacker sheet whereas the second is for a cell cut from a corner of the same sheet. The 9.9% reduction in short circuit current is accompanied by a 4.5% reduction in open circuit voltage. Such a change in V_{oc} cannot be accounted for by the change in I_{sc} alone. Since this change in I_{sc} could account for less than 1% in V_{oc}, one must look elsewhere to account for such a large change in V_{oc}.

2.3.2 Dark Current

A number of cell dark current densities have been plotted in Figure 13 through 15. Referring to the previous paragraph one should note the rather large difference in dark current between samples 13 and 21 of run W-13. The implication is that the recombination current in cell 21 appears to be considerably greater than is found for cell 13. In the same figure one can also examine the unusual dark current for control cell 2. In this instance the I-V curve indicates a shunt resistance of about 20 ohms. Dark current densities are listed in Table 2, appendix.

Dark currents are measured using a constant current supply in series with the device under test and a 1000 ohm resistor. Bias across the device is measured by a DVM and current is measured by a DVM across the 1000 ohm resistor.

2.3.3 Short Circuit Current and Open Circuit Voltage

Average value for short circuit current of cells made from Wacker Silso sheet material by the baseline method was determined and found to be 127 mA (2 cm x 2 cm) as opposed to the control

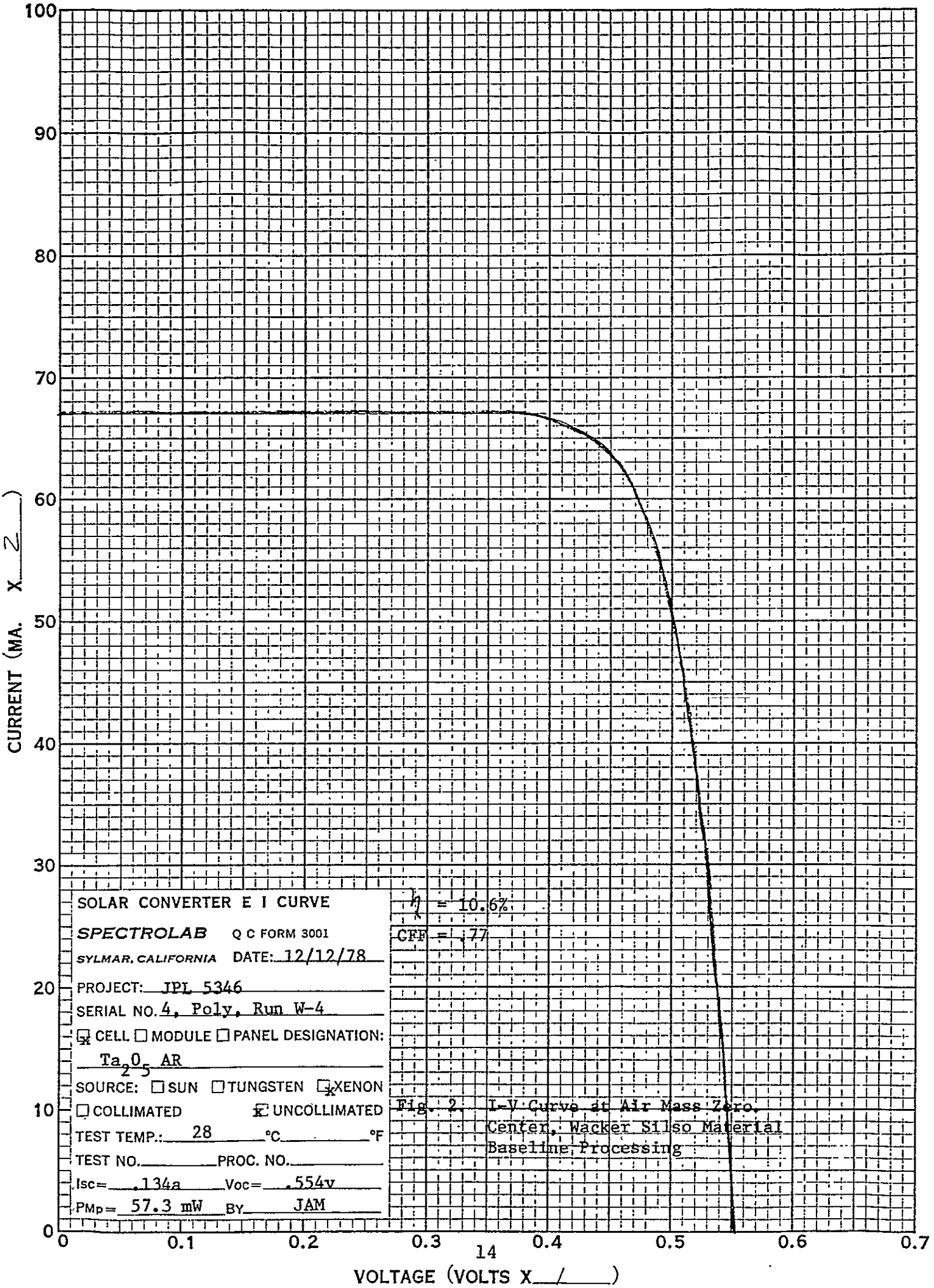

Fig. 2. I-V Curve at Air Mass Zero, Center, Wacker Silso Material Baseline Processing

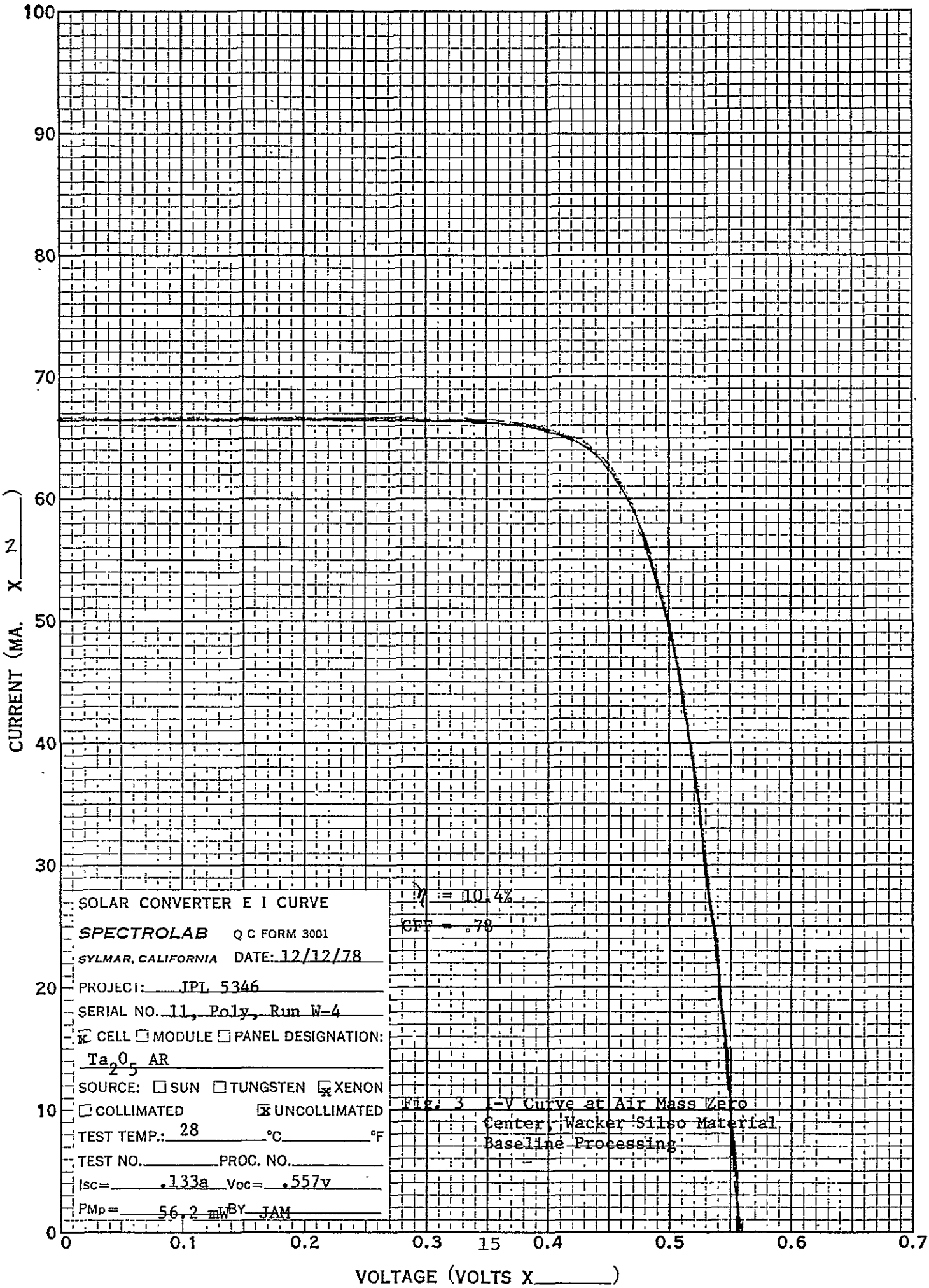

Fig. 3 I-V Curve at Air Mass Zero
Center, Wacker Silso Material
Baseline Processing

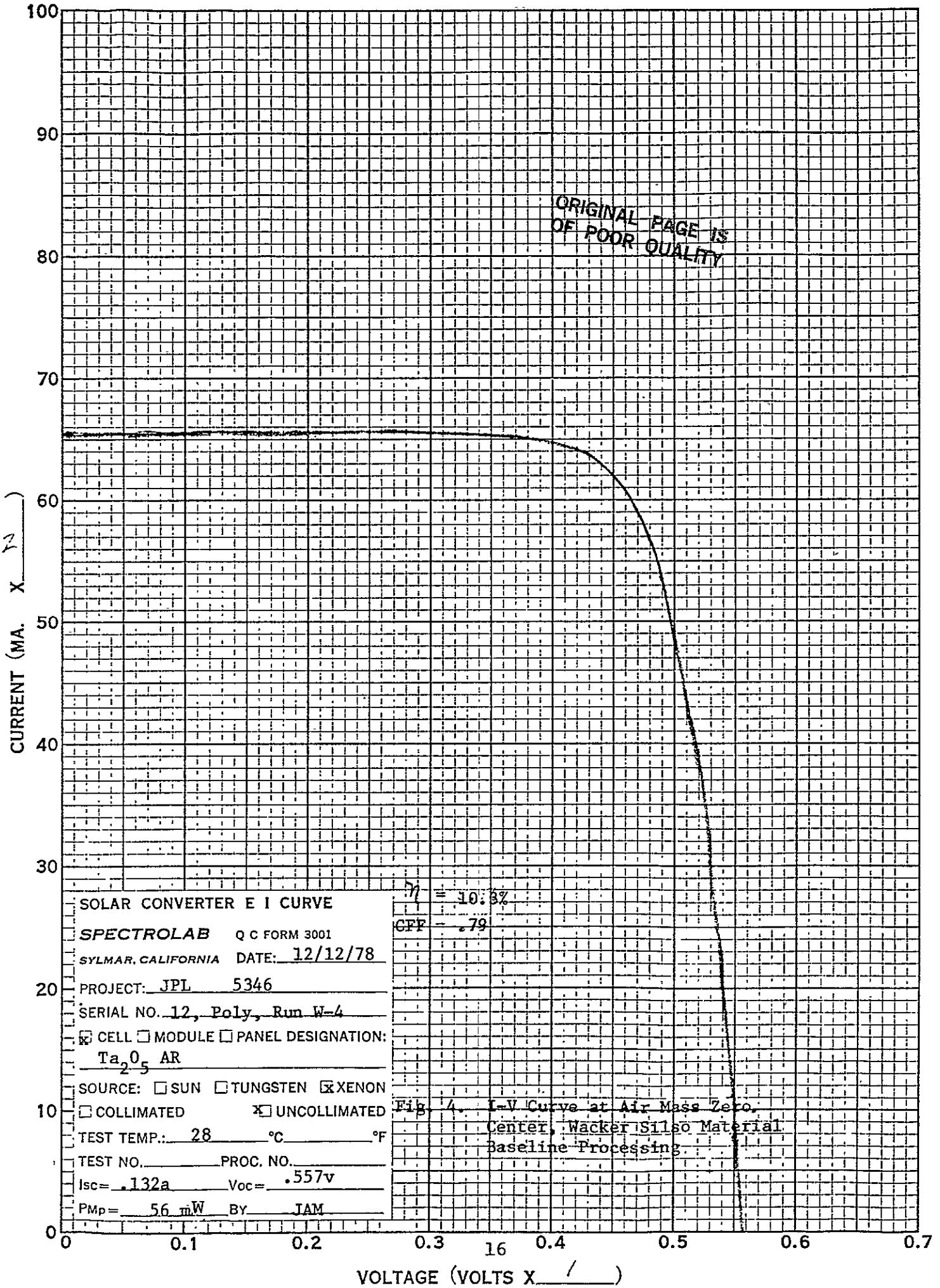

Fig. 4. I-V Curve at Air Mass Zero, Center, Wacker Silso Material Baseline Processing.

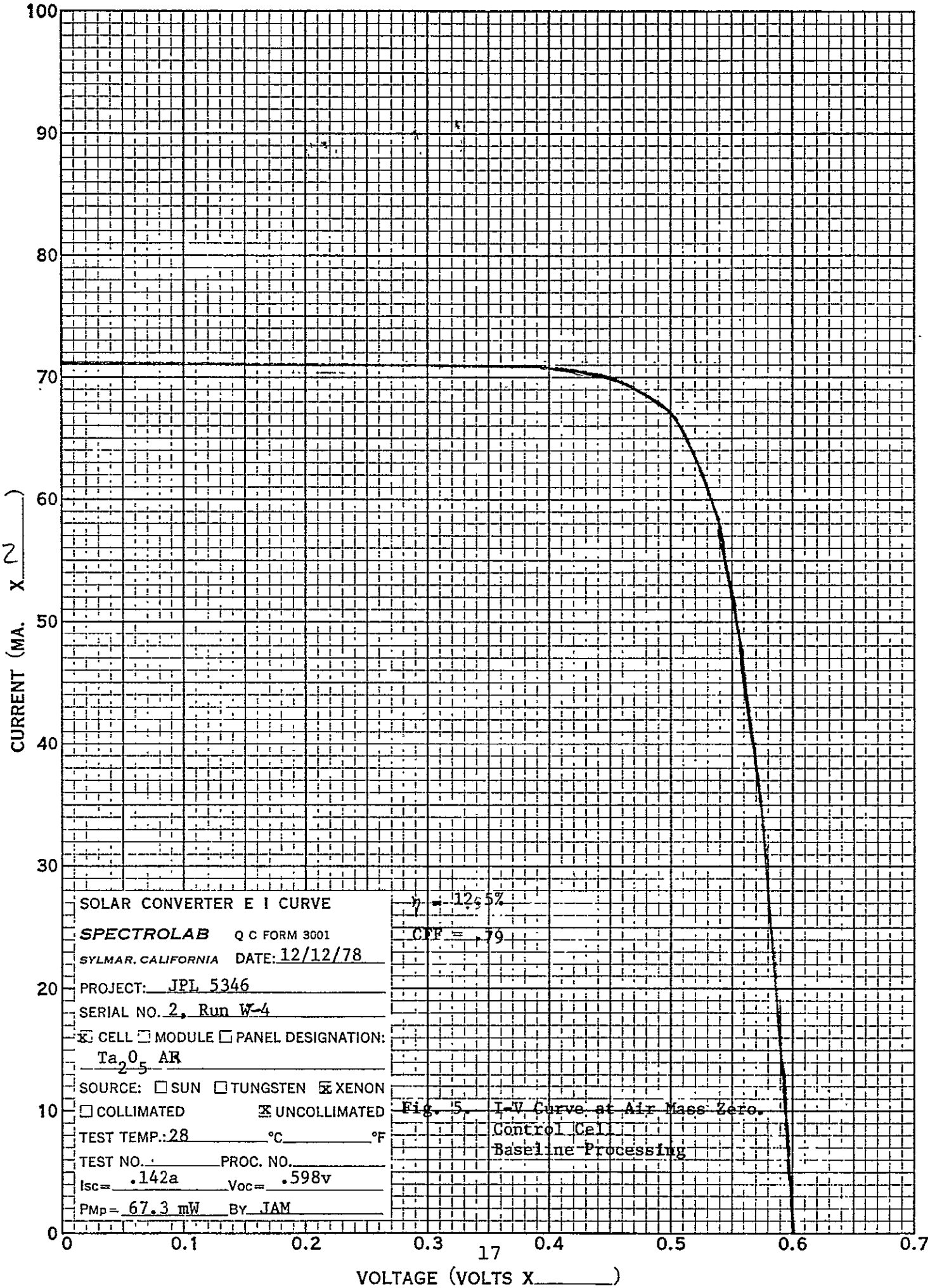

Fig. 5. I-V Curve at Air Mass Zero.
Control Cell
Baseline Processing

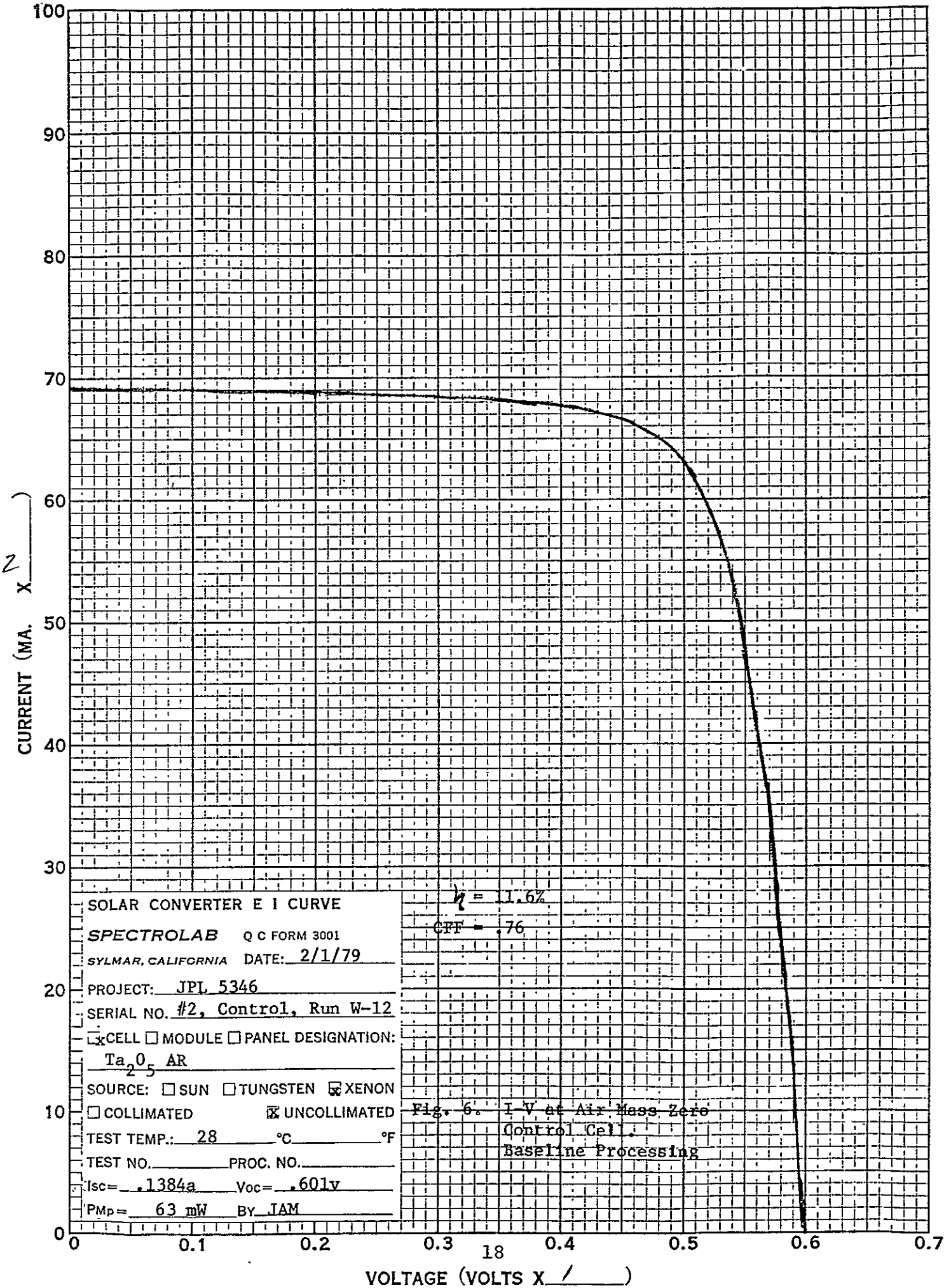

Fig. 6. I-V at Air Mass Zero
Control Cell,
Baseline Processing

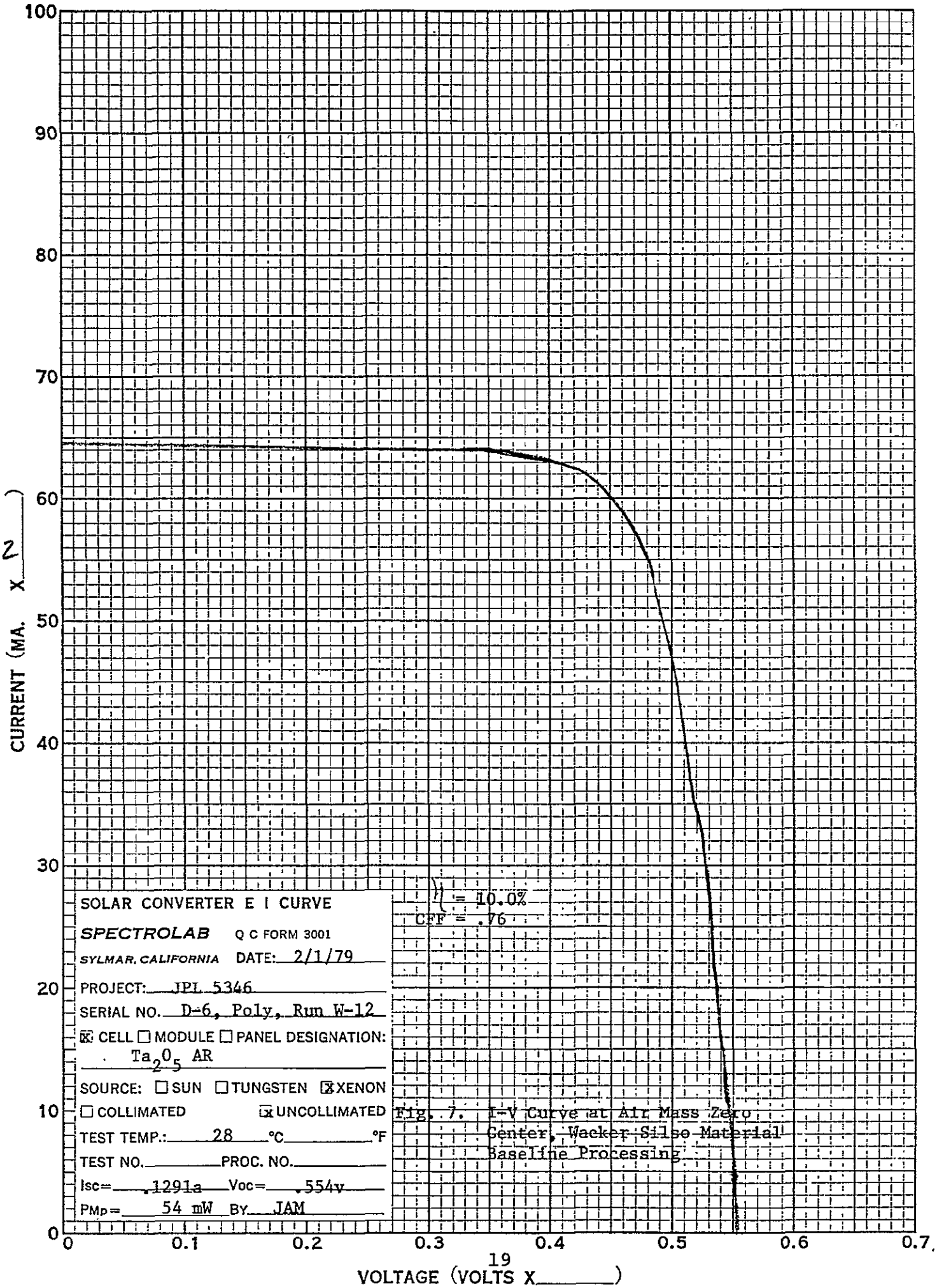

Fig. 7. I-V Curve at Air Mass Zero, Center, Wacker Silso Material, Baseline Processing

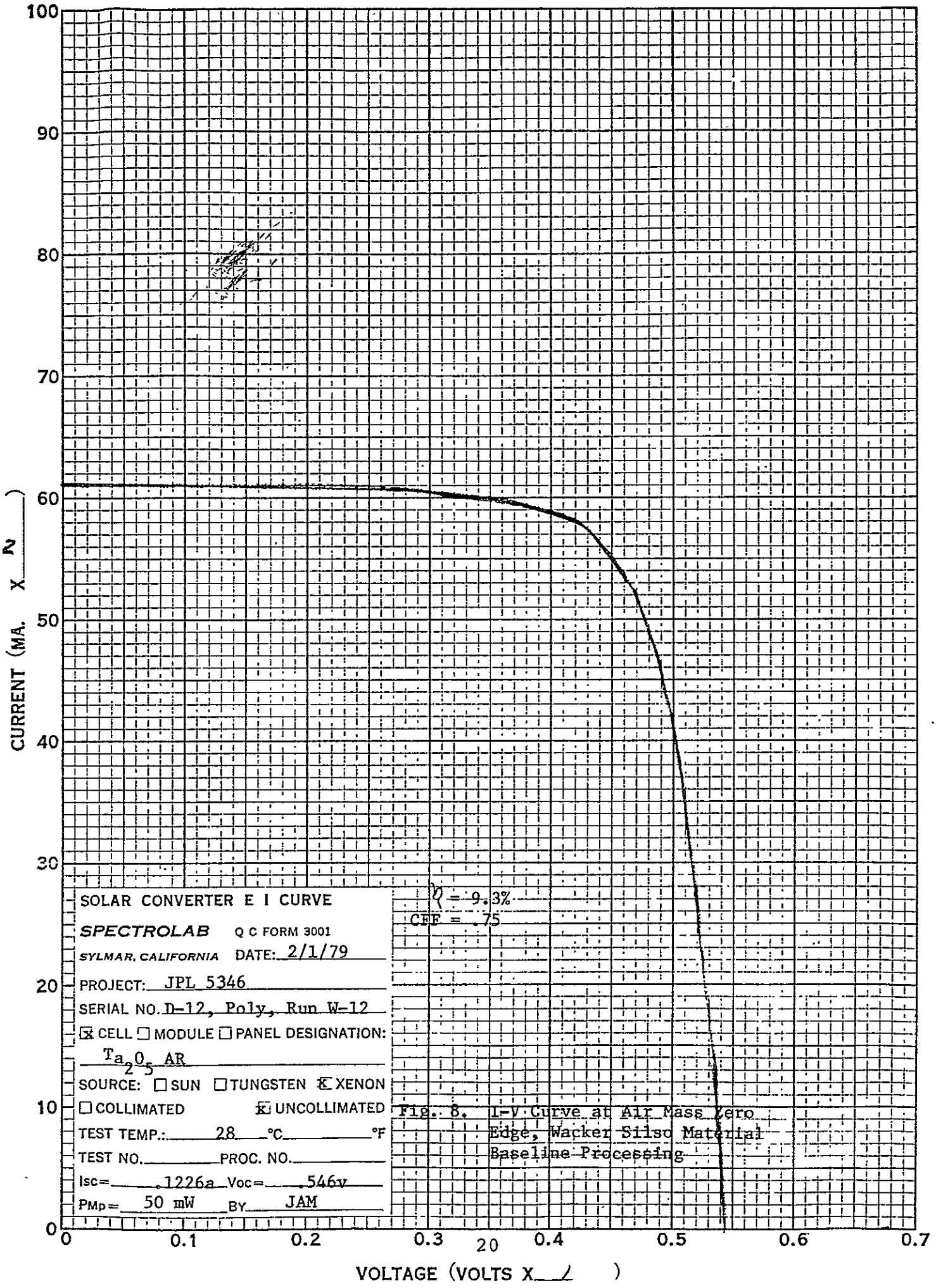

Fig. 8. I-V Curve at Air Mass Zero Edge, Wacker Silso Material Baseline Processing

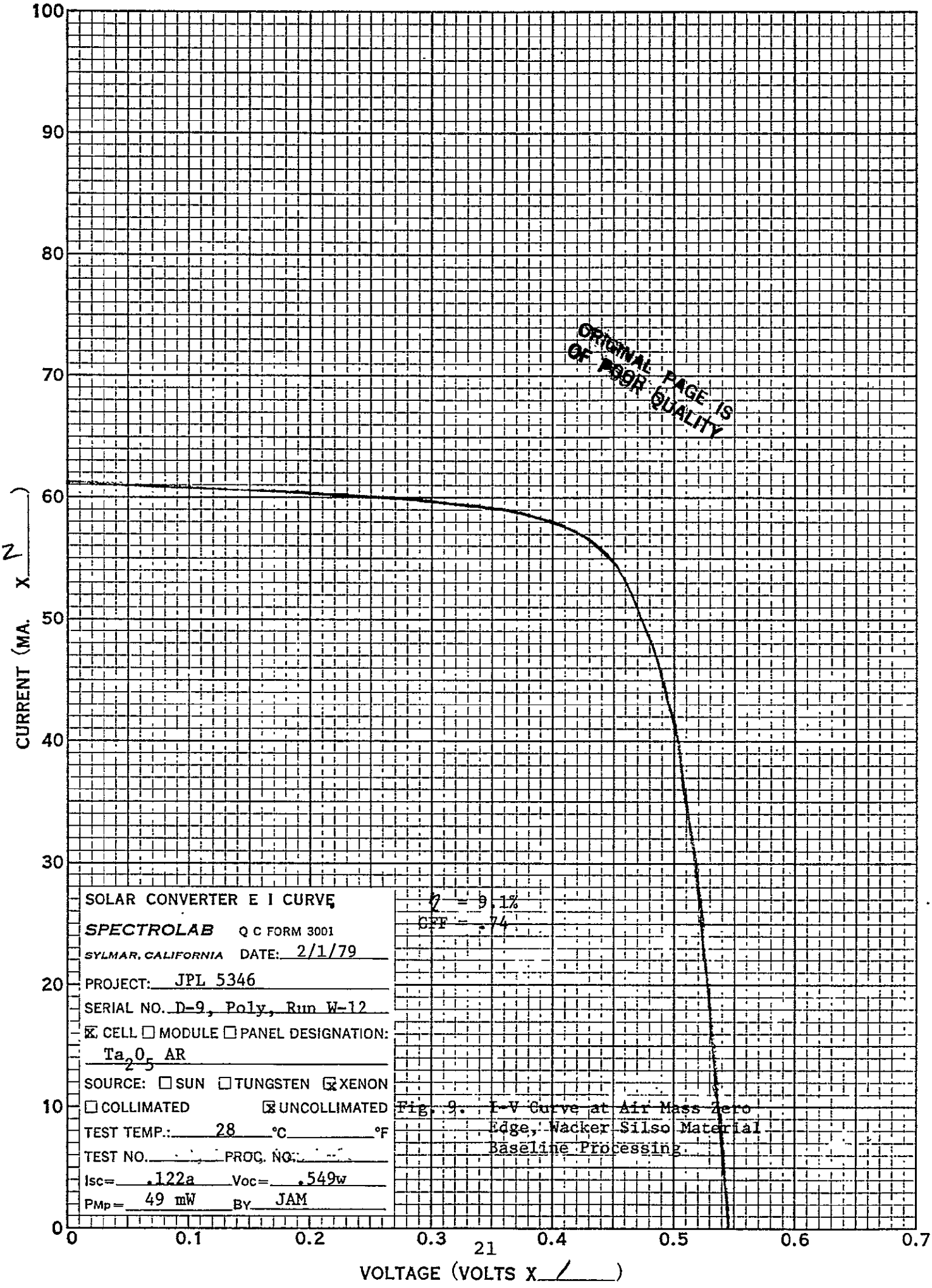

Fig. 9. I-V Curve at Air Mass Zero Edge, Wacker Silso Material Baseline Processing.

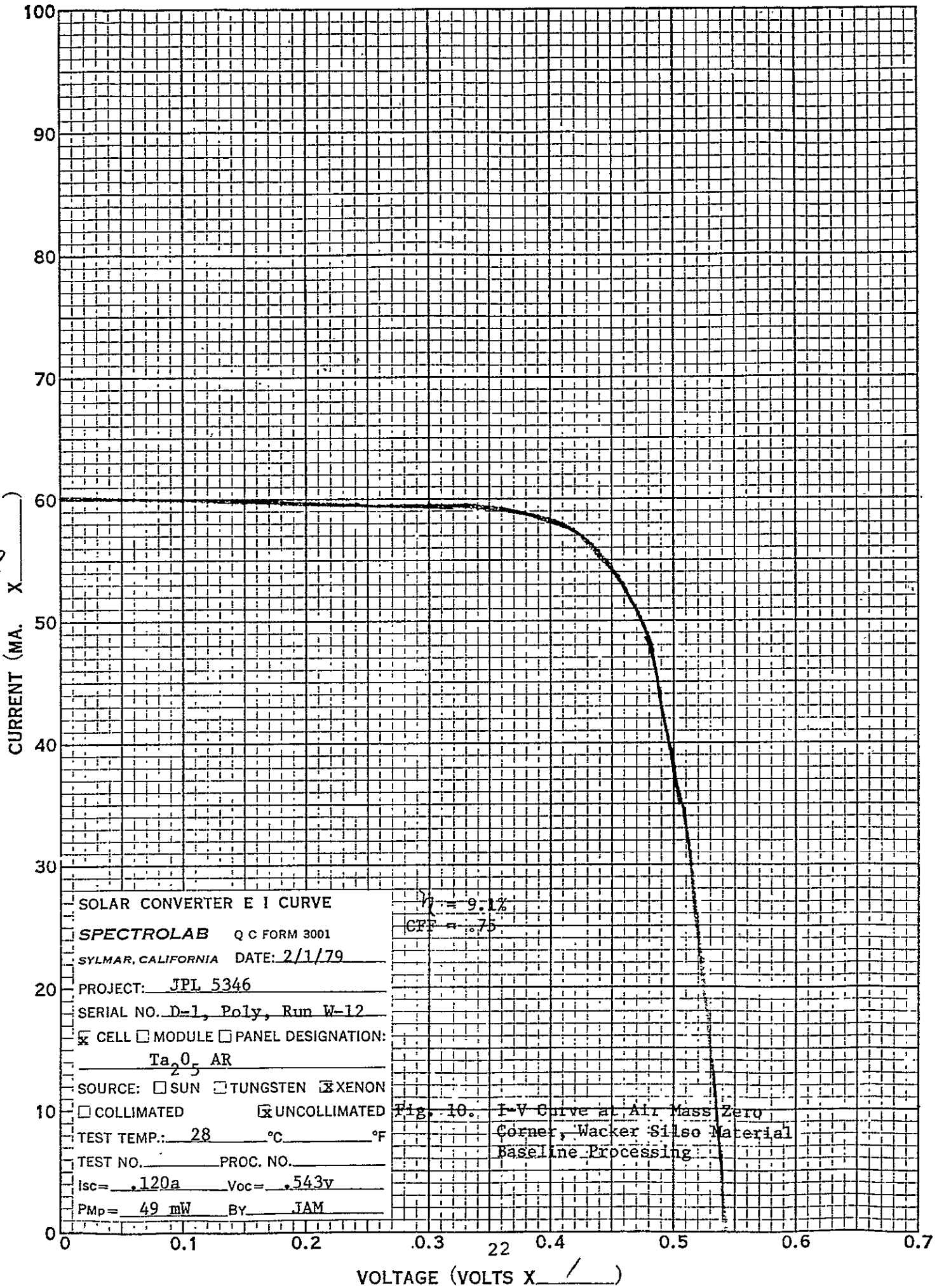

Fig. 10. I-V Curve at Air Mass Zero Corner, Wacker Silso Material Baseline Processing

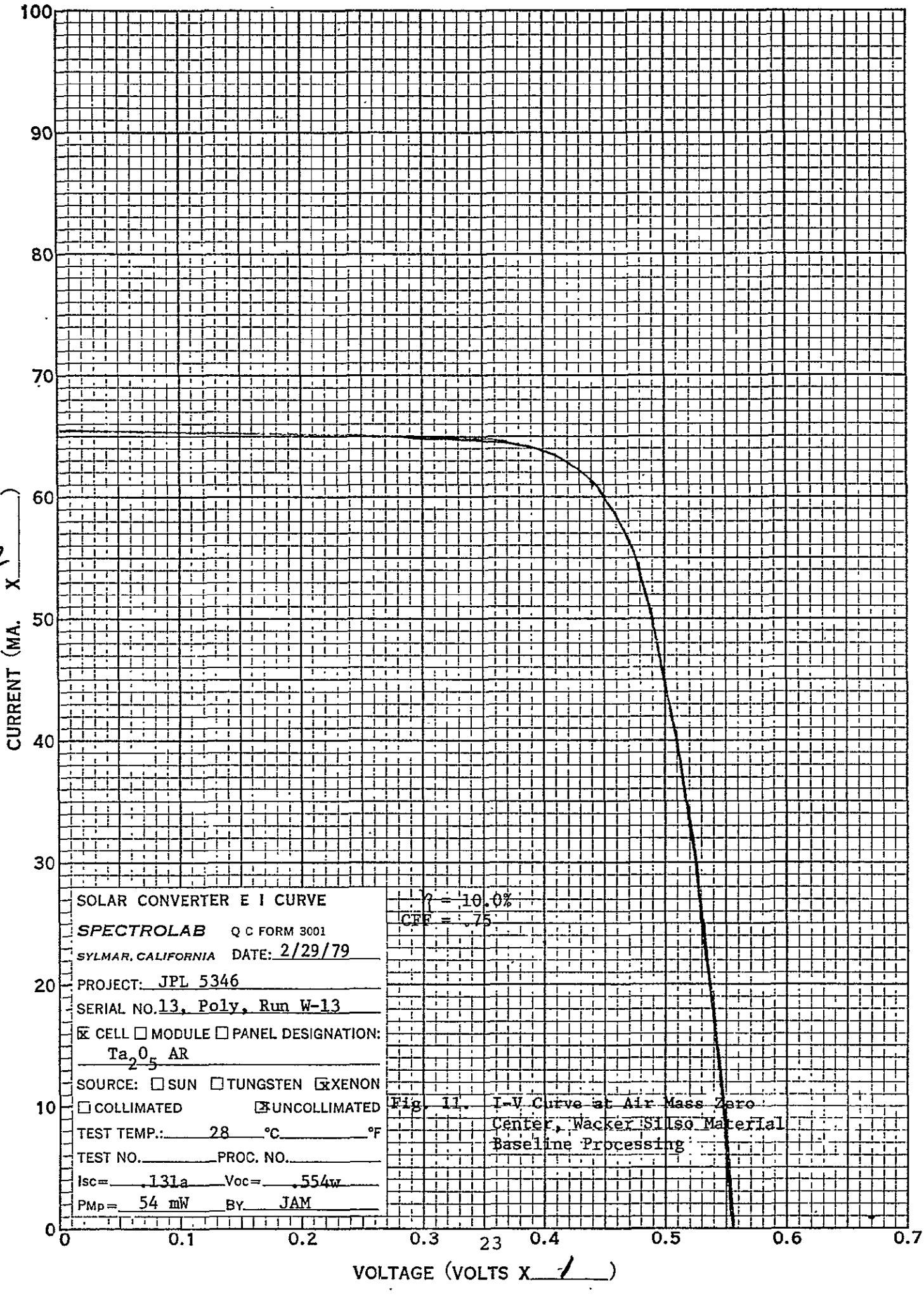

Fig. 11. I-V Curve at Air Mass Zero Center, Wacker Silso Material Baseline Processing

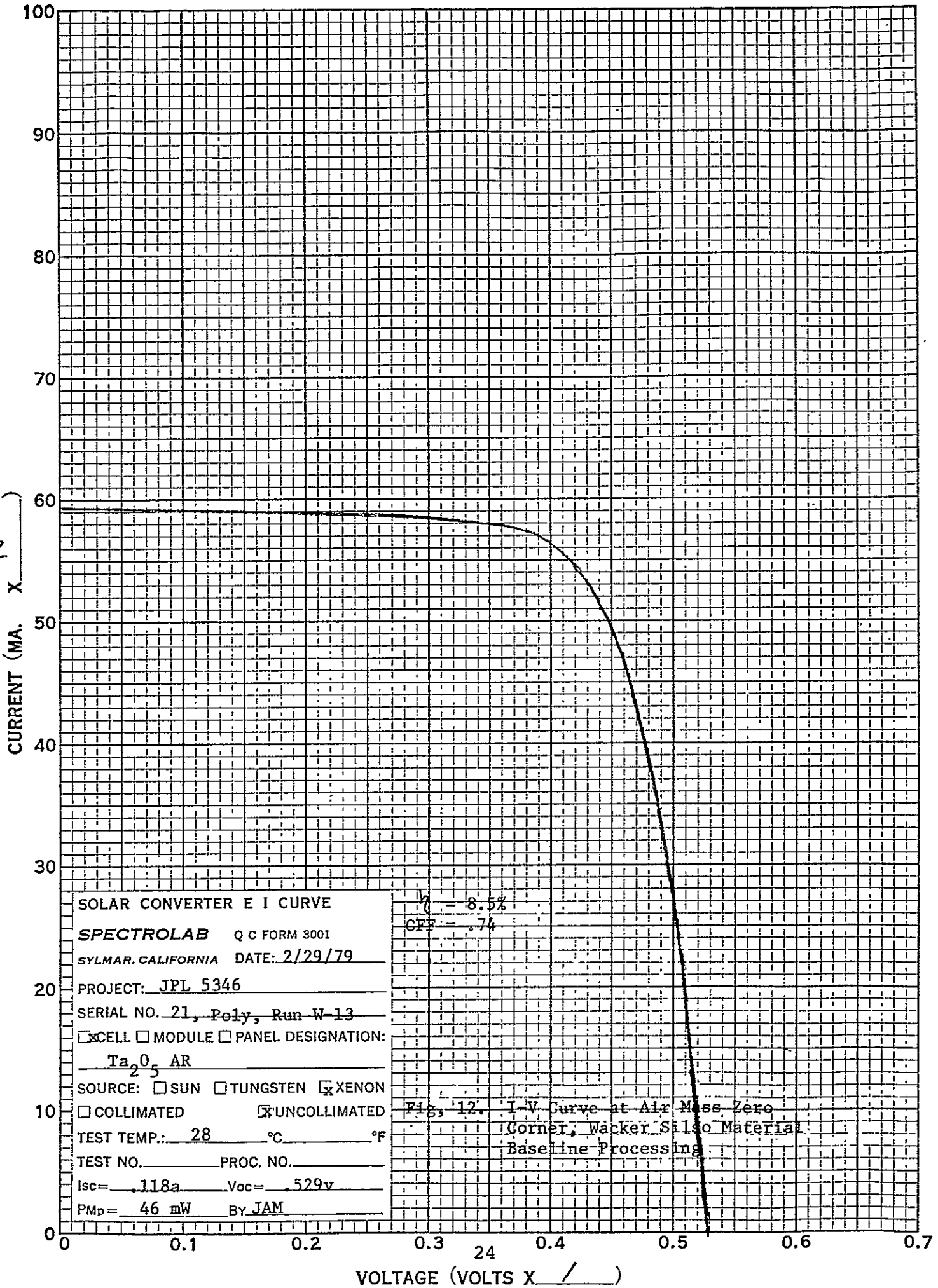

Fig. 12. I-V Curve at Air Mass Zero Corner, Wacker Silso Material Baseline Processing

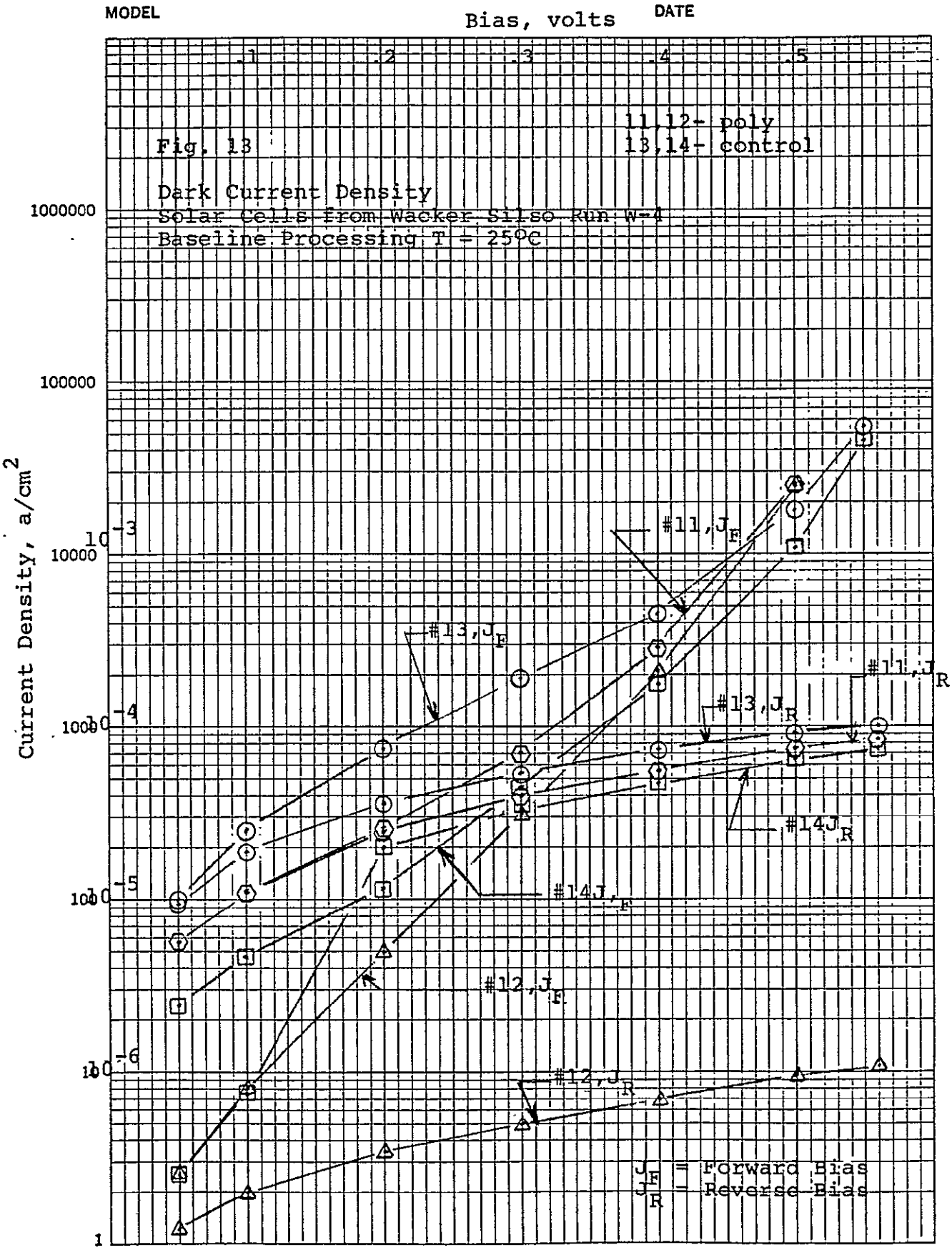
MODEL
Bias, volts
DATE
.1
.2
.3
.4
.5
11,12- poly
13,14- control
Fig. 13
Dark Current Density
Solar Cells from Wacker Silso Run W-4
Baseline Processing T = 25°C
1000000
100000
10000
1000
100
10
1
Current Density, a/cm2
10-3
10-4
10-5
10-6
#11,JF
#13,JF
#11,JR
#13,JR
#14JR
#14JF
#12,JF
#12,JR
JF = Forward Bias
JR = Reverse Bias

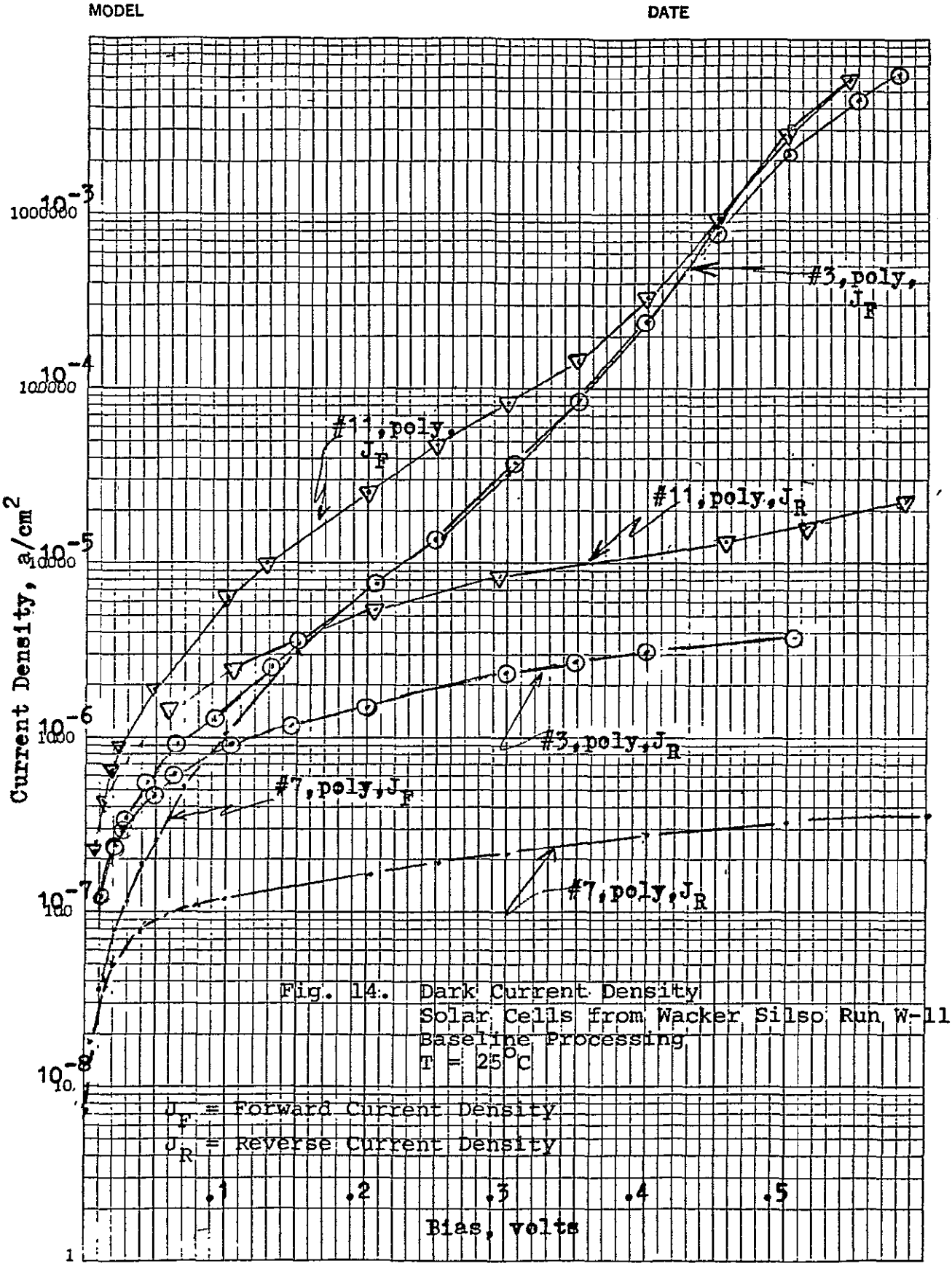

Fig. 14. Dark Current Density
Solar Cells from Wacker Silso Run W-11
Baseline Processing
T = 25°C

J_F = Forward Current Density
J_R = Reverse Current Density

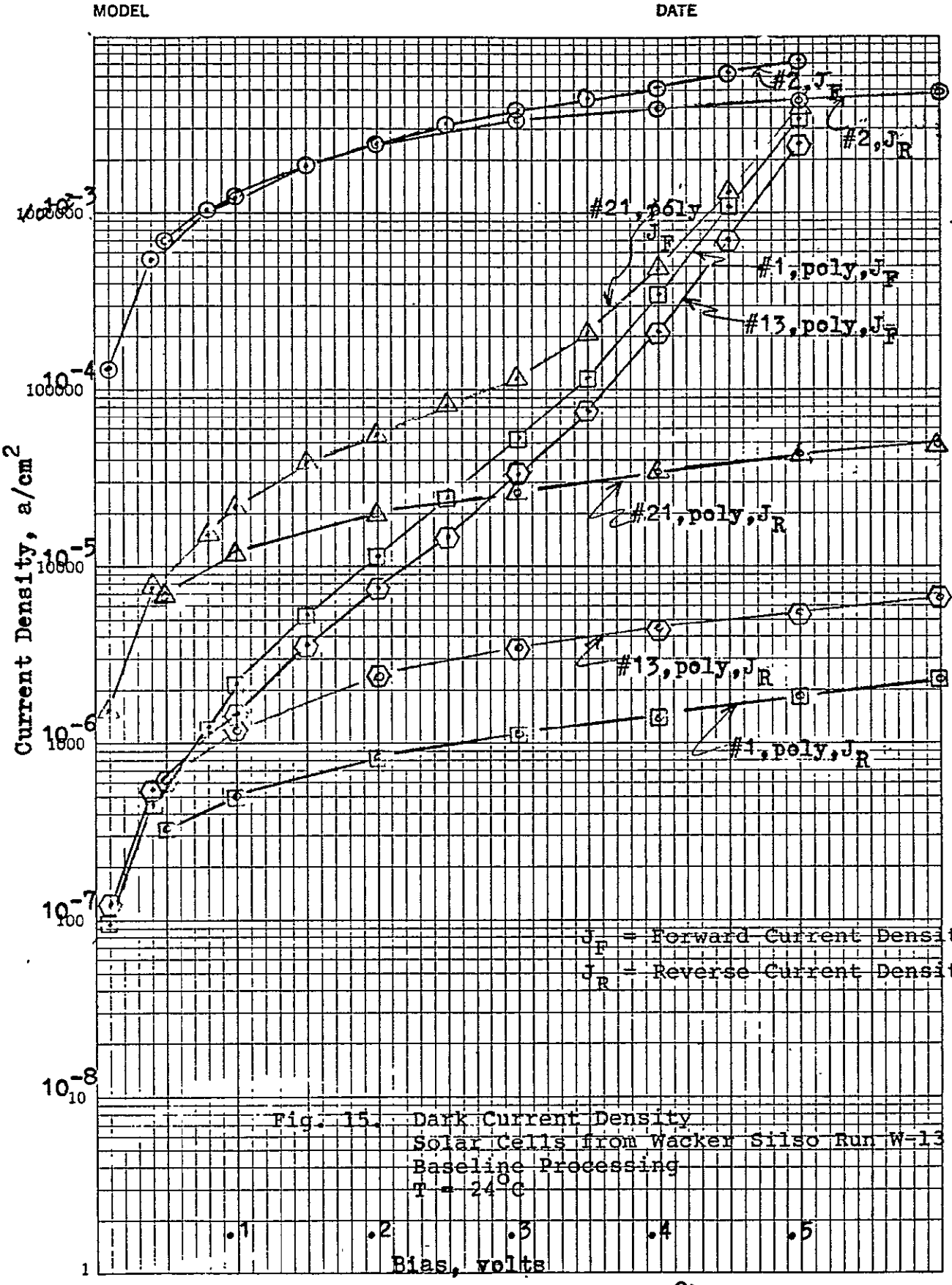

Fig. 15. Dark Current Density
Solar Cells from Wacker Silso Run W-13
Baseline Processing
T = 24°C

cells whose average short circuit current was found to be 139 mA. Open circuit voltage averages were found to be 546 mV for the Wacker (polycrystalline) cells and 598 mV for the control (single crystal) cells.

Measurements of these parameters were made on the Mark III solar simulator at air mass zero and 28°C.

2.3.4 Curve Fill Factor

These values have also been listed in Table 1 for all cells. Average value for the Wacker baseline cells was .74 whereas the average fill factor for the control baseline cells was .76. The fill factor was determined from the maximum power point on the I-V curve.

2.3.5 Efficiency

Efficiency values determined for each cell are listed in Table 1. The average value for all polycrystalline cells is 9.5% at AMO and 28°C. Average value for the control cells made by the same baseline process is 11.6%. The highest efficiency obtained in this study from a Wacker cell manufactured by the baseline process has been 10.6% while the highest efficiency for a control cell manufactured by the baseline process has been 12.5%.

Cell efficiency is based upon the total top surface area (2 cm x 2 cm) and an air mass zero irradiance of 135.3 mW/cm^2.

2.3.6 Spectral Response

Spectral response was measured on a system utilizing a filter wheel and cell holder having a controlled temperature. Cells were measured at 28°C. The filter wheel contained thirteen narrow bandpass filters with peaks at 400 nm to 1050 nm.

Irradiance at the measurement plane for each filter was determined by comparison with a calibrated solar cell. Results of these measurements are listed in Tables 8 through 11, appendix. Several spectral response curves are given in Figures 16, 17 and 18. These results show a continuing drop in sensitivity with increasing wavelength relative to the control cells.

III. Summary and Conclusions

Solar cells have been made by a baseline process using Wacker Silso polycrystalline sheet material. Efficiency has been shown to vary with position relative to the casting axis, with reduced efficiency toward outer regions of the sheet. This is probably a result of the direction of grain growth as found in these sheets. In the central core region grain growth appears to be in the direction of the casting axis whereas in the edge regions grain growth appears to be from the edge toward the center. This condition should lead to shorter effective diffusion lengths (reduced I_{sc}) and increased grain boundary density (increased saturation current) in the edge regions. Suppression of grain growth in edge regions of the casting should enhance polycrystalline cell efficiency if above model is accurate.

One might expect some improvement in efficiency at air mass zero by junctions shallower than those used in the baseline process, providing that increases in series resistance are minimized. Surface texturing, with effectiveness dependent upon individual grain orientation, would be expected to lead to some improvement, but less than the control cells with (100) orientation. The use of a back surface field could also lead to increased efficiency. It should be most effective in the central regions and of minimal effectiveness in the edge region of the sheet where grain boundaries will occupy planes between the depletion region and the

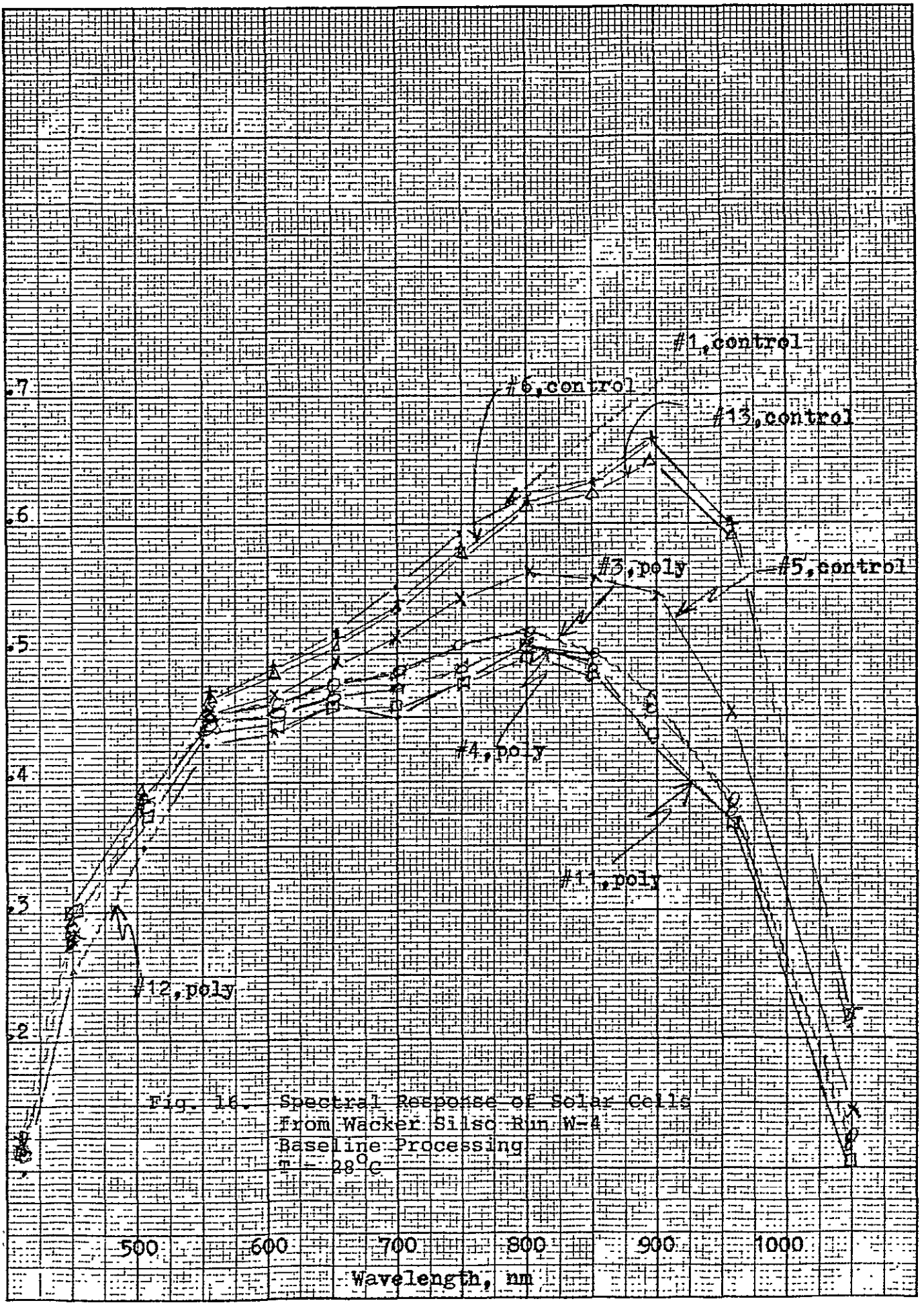

Fig. 16. Spectral Response of Solar Cells From Wacker Silso Run W-4 Baseline Processing T = 28°C

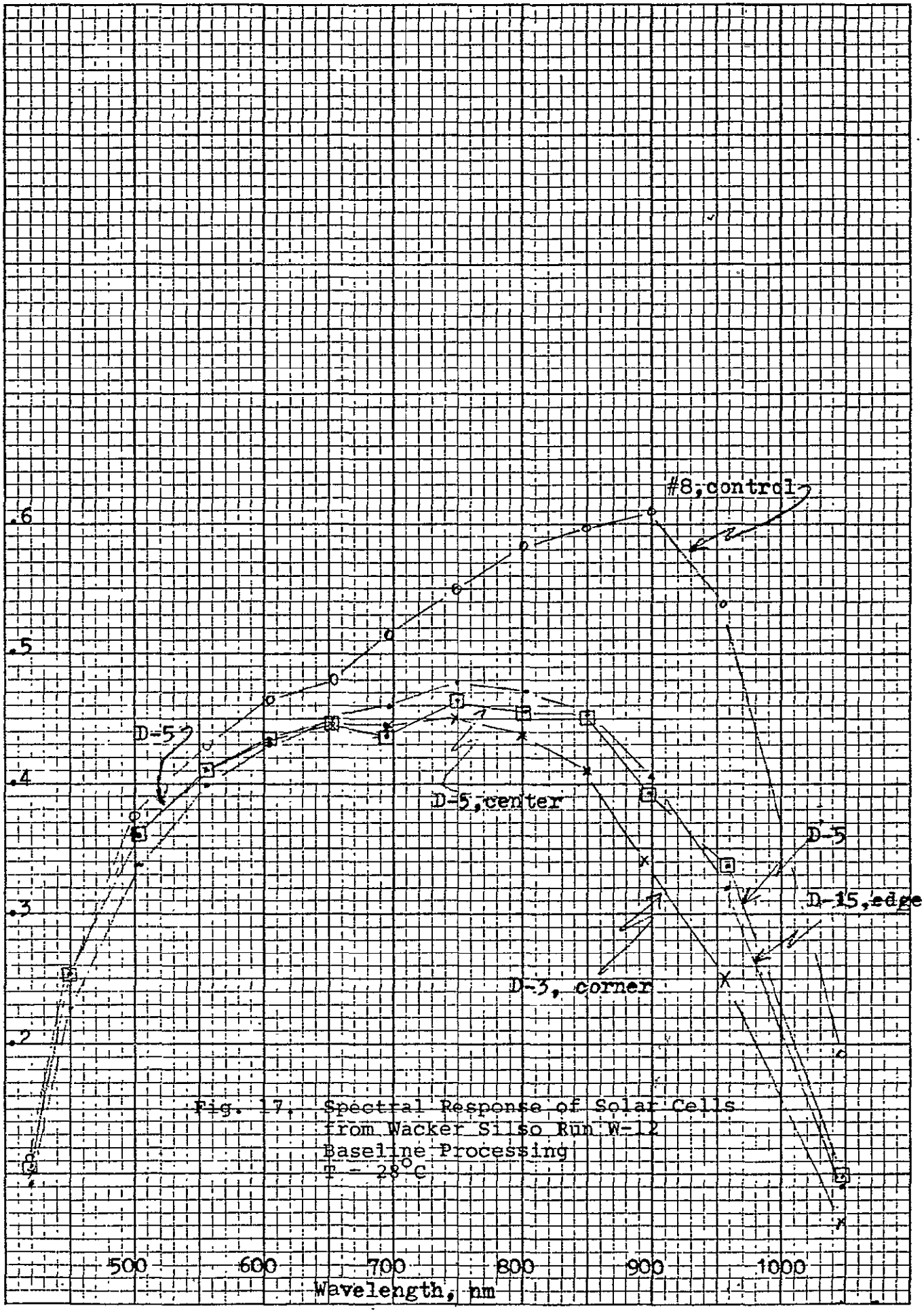

Fig. 17. Spectral Response of Solar Cells from Wacker Silso Run W-12 Baseline Processing $T = 28^{\circ}C$

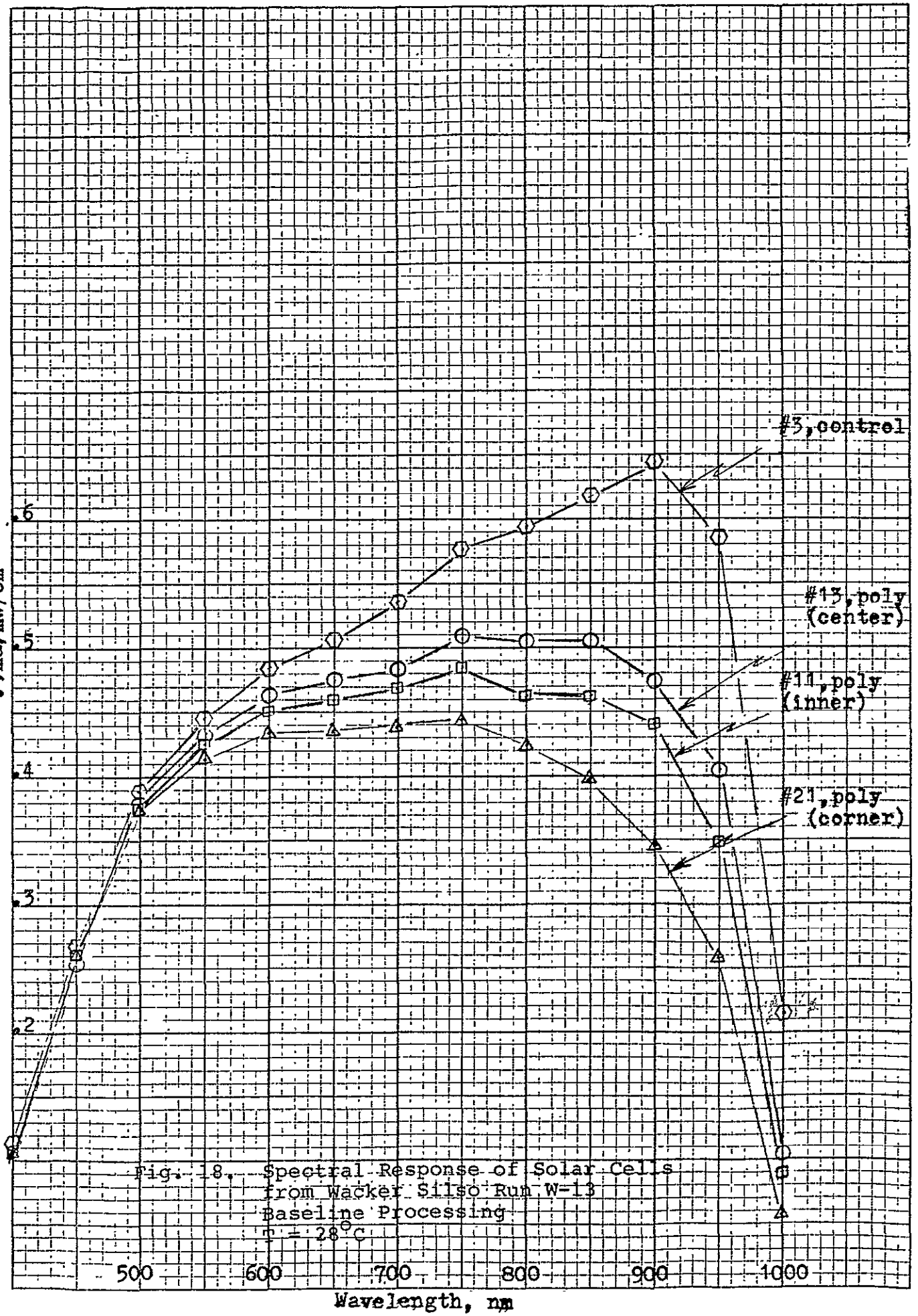

Fig. 18. Spectral Response of Solar Cells from Wacker Silso Rum W-13 Baseline Processing $T = 28^{\circ}C$

back contact. Various complications can arise because of the density of grain boundaries whose properties for either diffusion or melt-regrowth differ markedly from the bulk.

Results for the Wacker material fabricated by the baseline process have been relatively good, especially when one considers the large number of grain boundaries included in each cell. Handling of the wafers did not present any difficulties. In the initial work it was noted that fracture was occurring along grain boundaries, as would be expected, but no extraordinary measures were required to minimize fracture. From the results shown in several of the runs it should be possible to make large area cells without degradation and obtain the maximum packing allowed by the rectangular shape. The material should be readily adaptable to less expensive processing methods, such as screen printed contacts.

IV. Recommendations

To determine a more effective processing regime for the Wacker material several strategies should be investigated. The first of these is to reduce the depth of the diffused junction. Any reduction in junction depth will increase the collection of short wavelength generated minority carriers to a large extent and less so for the long wavelength generated minority carriers. Reduced junction depth will, of course, lead to increased sheet resistance that must be balanced by a greater gridline density. Surface texturizing to reduce surface reflection will also improve the cell efficiency. The effectiveness of this will depend upon the orientation of the individual grains. Finally, application of a back surface field would be expected to offer some improvement in cells cut from the center region. Cells cut from the outer edge might be less affected by the back surface field owing to the grain geometry.

Although the contract had a rather slow beginning rapid progress was made in the closing days of the quarter. This is expected to increase in the weeks ahead by the use of additional personnel coupled with parallel processing of materials in both the baseline and optimized regime.

V. Work Projected for Next Quarter

In the coming quarter, in addition to the optimized processing of Wacker material, we plan to complete baseline processing of Web, RTR, HEM, and EFG grown materials. Optimized processing will also be initiated on several of the above. Pending delivery of instrumentation, we hope to have systems in place for diffusion length, logarithmic dark current, and scanning light spot measurements.

A P P E N D I X

Table 5

Dark Current Run W-4, Temp. 24°C

$I_{F,R}$, a/cm^2

V/F volts	1*	2*	3*	4	5*	6*	9*
.05	1.25×10^{-6}	1.0×10^{-6}	2.5×10^{-8}	5×10^{-7}	1.9×10^{-6}	7.5×10^{-7}	5×10^{-7}
.10	4.0	2.5	4×10^{-6}	1×10^{-6}	5.4	1.9×10^{-6}	1.5×10^{-6}
.20	1.6×10^{-5}	1.4×10^{-5}	1.1×10^{-5}	4	1.8×10^{-5}	8.5	8
.30	6.0	5.2	3.5	2.3×10^{-5}	4.9	3.3×10^{-5}	2.5×10^{-5}
.40	2.2×10^{-4}	2.0×10^{-4}	1.1×10^{-4}	2×10^{-4}	1.7×10^{-4}	1.3×10^{-4}	8.8
.50	1.3×10^{-3}	1.2×10^{-3}	2.7×10^{-4}	2.7×10^{-3}	1.1×10^{-3}	9.4	7.6×10^{-4}
.56	5.4	5.0	3.9×10^{-4}		4.1	4.7×10^{-3}	5.1×10^{-3}

	10*	11	12	13*	14*
.05	7.5×10^{-7}	5.8×10^{-6}	2.5×10^{-7}	1.0×10^{-5}	2.5×10^{-6}
.10	3.0×10^{-6}	1.1×10^{-5}	8.0	2.5	4.8
.20	1.8×10^{-5}	2.7	5.0×10^{-6}	7.4	1.2×10^{-5}
.30	6.5	7.0	3.2×10^{-5}	1.9×10^{-4}	4.5
.40	2.1×10^{-4}	2.9×10^{-4}	2.1×10^{-4}	4.6	1.8×10^{-4}
.50	1.1×10^{-3}	2.6×10^{-3}	2.6×10^{-3}	1.8×10^{-3}	1.1×10^{-3}
.56	5.1			5.6	3.7

V/R	1*	2*	3*	4	5*	6*	9*
.05	1×10^{-6}	7.5×10^{-7}	1.8×10^{-6}	2.3×10^{-7}	1.1×10^{-6}	7.5×10^{-7}	4.8×10^{-7}
.1	2.3	1.3×10^{-6}	4×10^{-6}	3.8	1.6	1.5×10^{-6}	5.0
.2	4.8	2.3	7.3×10^{-6}	5.8	2.3	2.8	7.3
.3	5.8	3.5	1.2×10^{-5}	7.8	2.9	4.3	1.0×10^{-6}
.4	7.5	4.8	1.6×10^{-5}	9.8	3.4	5.5	1.0
.5	8.5	6	2.1×10^{-5}	1.2×10^{-6}	4.0	7	1.3
.56		6.8	2.4×10^{-5}	1.3	4.3	7.8	1.5

	10*	11	12	13*	14*
.05	5.0×10^{-7}	5.5×10^{-6}	1.3×10^{-7}	9.3×10^{-6}	2.5×10^{-7}
.1	5.0	1.2×10^{-5}	2.0	1.9×10^{-5}	7.5×10^{-5}
.2	7.5	2.6	3.5	3.7	2.0×10^{-5}
.3	7.5	4.0	5.0	5.4	3.4
.4	1.0×10^{-6}	5.6	7.0	7.3	4.8
.5	1.3	7.3	9.5	9.1	6.5
.56	1.3	8.3	1.1×10^{-6}	1.0×10^{-4}	7.4

*Control cell

Table 6

Dark Current Density Run W-12, Temp. 24°C

I_F, a/cm^2

V/F volts	1*	4*	5*	A-1	D-1	D-2	D-3
.01	2.8×10^{-6}	1.2×10^{-6}	5×10^{-9}	5×10^{-9}	3.3×10^{-6}	1.4×10^{-6}	1.1×10^{-5}
.04	1.2×10^{-5}	7.1	5.0	1×10^{-8}	1.2×10^{-5}	7.7	4.6
.08	3.0	2.5×10^{-5}	7.5	2.5	2.5	1.5×10^{-5}	1.0×10^{-4}
.10	4.1	4.0	7.5		3.2	1.9	1.3
.15	7.8	9.0	1.0×10^{-8}	4.5	4.9	3.0	2.1
.20	1.3×10^{-4}	1.6×10^{-4}	1	5.8	6.9	4.4	3.1
.25	2.0	2.6	1.3	7.5	9.6	6.1	4.1
.30	2.9	3.8	1.5	9	1.4×10^{-4}	8.1	5.2
.35	4.0	5.3	1.5	1.0×10^{-7}	2.2	1.2×10^{-4}	6.8
.40	5.5	7.4	3.7×10^{-4}	1.2	4.4	1.8	9.7
.45	8.1	1.1×10^{-3}	9.4	1.3	1.2×10^{-3}	2.6	1.9×10^{-3}
.50	1.4×10^{-3}	2.0		1.4	4.0	3.8	5.2

V/F volts	D-4	D-5	D-7	D-8	D-11
.01	5×10^{-8}		3.7×10^{-7}	8.8×10^{-7}	4.5×10^{-7}
.04	2.2×10^{-7}	3×10^{-8}	1.4×10^{-6}	4.6×10^{-6}	1.9×10^{-6}
.08	6.3		2.9	1.3×10^{-5}	4.4
.10	9.8	5.8	3.6	1.8	5.9
.15	2.7×10^{-6}	5.6	3.5	1.1×10^{-5}	
.20	6.4	4.2×10^{-7}	8.3	5.9	2.0
.25	1.3×10^{-5}		1.3×10^{-5}	9.1	3.4
.30	2.4	1.8×10^{-6}	2.3	1.4×10^{-4}	6.1
.35	4.1		5.4	2.2	1.2×10^{-4}
.40	6.7	5.1	1.6×10^{-4}	4.4	3.0
.45	1.1×10^{-4}		4.4	9.6	9.3
.50	1.5	1.3×10^{-5}	1.3×10^{-3}	2.8×10^{-3}	3×10^{-3}

*Control cells

Dark Current Density I_R, a/cm^2

Run W-12, Temp. 24°C continued

V/R volts	1*	4*	5*	A-1	D-1	D-2	D-3
.05	$1.6x10^{-5}$	$2.6x10^{-6}$	$3.7x10^{-7}$	$7.5x10^{-9}$	$1.5x10^{-5}$	$9.3x10^{-6}$	$4.2x10^{-5}$
.1	2.4	3.4	9.5	$1.3x10^{-8}$	3.1	$2.0x10^{-5}$	6.8
.2	4.7	4.3	$2.5x10^{-6}$	5.3	6.2	3.8	9.5
.3	7.0	5.1	4.6	$1.5x10^{-7}$	9.4	5.8	$1.1x10^{-4}$
.4	9.2	5.8	6.2	4.8	$1.3x10^{-4}$	7.8	1.3
.5	$1.2x10^{-4}$	6.6	9.7	$1.6x10^{-6}$	1.6	9.9	1.4
.6	1.4	7.4	$1.3x10^{-5}$	4.5	1.9	$1.2x10^{-4}$	1.5

	D-4	D-5	D-7	D-8	D-11
.05	$1.7x10^{-7}$	$1x10^{-8}$	$1.9x10^{-6}$	$2.4x10^{-6}$	$2.0x10^{-6}$
.1	2.8	1.5	3.8	3.4	3.7
.2	4.7	2.5	8.1	4.3	7.1
.3	6.6	3.5	$1.3x10^{-5}$	5.0	$1.1x10^{-5}$
.4	8.4	4.3	1.8	5.7	1.4
.5	1.0	4.3	2.0	6.4	1.7
.6	1.2		2.6	6.9	2.2

*Control cells

Table 7

Dark Current $I_{F,R}$, a/cm^2 Run W-13, Temp. 25°C

V/F	2	4	6	7	8
.01	6.8×10^{-7}	2.5×10^{-8}	1.0×10^{-5}	3.1×10^{-7}	2.8×10^{-8}
.04	3.2×10^{-6}	1.2×10^{-7}	4.1	1.3×10^{-6}	1.2×10^{-7}
.08	7.7	3.8	8.4	3.0	3.4
.10	1.1×10^{-5}	6.3	1.1×10^{-4}	4.1	5.4
.15	2.1	1.9×10^{-6}	1.6	7.8	1.5×10^{-6}
.20	3.9	4.9	2.2	1.4×10^{-5}	3.7
.25	6.6	1.2×10^{-5}	2.8	2.5	9.5
.30	1.1×10^{-4}	3.0	3.7	4.7	2.5×10^{-5}
.35	2.0	8.5	5.0	9.5	7.0
.40	4.2	2.8×10^{-4}	7.9	2.4×10^{-4}	2.2×10^{-4}
.45	1.2×10^{-3}	1.0×10^{-3}	1.7×10^{-3}	7.7	7.7
.50	3.4	3.4	4.6	2.7×10^{-3}	2.6×10^{-3}
V/R					
.05	2.9×10^{-6}	7.3×10^{-8}	4.8×10^{-5}	1.5×10^{-6}	7.8×10^{-8}
.1	5.4	1.1×10^{-7}	9.2	3.0	1.2×10^{-7}
.2	1.0×10^{-5}	1.6	1.6×10^{-4}	6.3	2.0
.3	1.4	2.0	2.2	9.9	2.9
.4	1.8	2.5	2.7	1.4×10^{-5}	3.8
.5	2.2	2.7	3.1	1.8	4.8
.6	2.7	3.1	3.5	2.2	6.1

Dark Current

$I_{F,R}$, a/cm^2

Run W-13, Temp. 25°C
continued

V/F	11	12	13	14	16	17	18	19
.01	8.8×10^{-8}	2.0×10^{-8}	1.3×10^{-7}	3.8×10^{-8}	3.4×10^{-7}	1.1×10^{-6}	1.8×10^{-8}	3.0x10-8
.04	3.9×10^{-7}	8.3	5.5	1.7×10^{-7}	1.5×10^{-6}	4.4	7.0	1.3×10^{-7}
.08	9.9	2.4×10^{-7}	1.2×10^{-6}	4.6	3.5	8.9	2.0×10^{-7}	4.0
.10	1.4×10^{-6}	3.9	1.7	6.7	4.7	1.1×10^{-5}	3.1	6.2
.15	3.1	1.1×10^{-6}	3.6	1.6×10^{-6}	8.6	1.7	8.6	1.7×10^{-6}
.20	6.4	3.0	7.7	3.6	1.5×10^{-5}	2.4	2.3×10^{-6}	4.4
.25	1.4×10^{-5}	7.6	1.6×10^{-5}	8.9	2.6	3.4	6.4	1.0×10^{-5}
.30	3.1	2.0×10^{-5}	3.4	2.3×10^{-5}	4.9	5.1	1.8×10^{-5}	2.5
.35	8.4	5.7	7.7	6.6	1.1×10^{-4}	9.4	5.5	6.7
.40	2.8×10^{-4}	1.9×10^{-4}	2.1×10^{-4}	2.1×10^{-4}	3.4	2.5×10^{-4}	1.9×10^{-4}	2.2×10^{-4}
.45	1.0×10^{-3}	7.2	7.0	8.2	1.2×10^{-3}	8.9	7.6	8.2
.50	3.5	2.7×10^{-3}	2.5×10^{-3}	3.3×10^{-3}	3.9	3.3×10^{-3}	2.8×10^{-3}	3.1×10^{-3}
V/R								
.05	3.3×10^{-7}	5.5×10^{-8}	6.2×10^{-7}	1.3×10^{-7}	3.1×10^{-7}	5.4×10^{-6}	5.3×10^{-8}	9.3×10^{-8}
.1	5.5	8.8	1.2×10^{-6}	2.1	2.2×10^{-6}	1.1×10^{-5}	8.0	1.4×10^{-7}
.2	8.8	1.4×10^{-7}	2.4	3.3	3.0	2.1	1.3×10^{-7}	2.2
.3	1.2×10^{-6}	2.0	3.5	4.4	3.5	3.2	1.6	2.8
.4	1.5	2.7	4.6	5.4	3.9	4.2	2.0	3.4
.5	1.9	3.3	5.7	6.4	4.3	5.3	2.3	4.0
.6	2.3	4.1	6.8	7.5	4.6	6.3	2.7	4.5

Dark Current

Run W-13, Temp. 25°C
continued

$I_{F,R}$, a/cm^2

V/F	21	22	24	25
.01	$1.7x10^{-6}$	$3.5x10^{-6}$	$1.8x10^{-6}$	$2.1x10^{-6}$
.04	$7.5x10^{-6}$	$1.4x10^{-5}$	$7.8x10^{-6}$	8.4
.08	$1.7x10^{-5}$	3.1	$1.8x10^{-5}$	$1.7x10^{-5}$
.10	$2.2x10^{-5}$	4.0	2.4	2.1
.15	$3.8x10^{-5}$	6.8	4.1	3.3
.20	$5.6x10^{-5}$	$1.0x10^{-4}$	6.2	4.7
.25	$8.1x10^{-5}$	1.5	6.5	6.5
.30	$1.2x10^{-4}$	2.3	$1.3x10^{-4}$	9.4
.35	$2.1x10^{-4}$	3.5	2.1	$1.5x10^{-4}$
.40	$4.9x10^{-4}$	6.6	4.3	2.5
.45	$1.4x10^{-3}$	$1.7x10^{-3}$	$1.2x10^{-3}$	4.2
.50	$3.9x10^{-3}$	4.7	2.9	6.6
V/R				
.05	$6.9x10^{-6}$	$1.6x10^{-5}$	$7.1x10^{-6}$	$1.0x10^{-5}$
.1	$1.2x10^{-5}$	3.3	$1.2x10^{-5}$	2.1
.2	$2.0x10^{-5}$	6.4	1.8	4.2
.3	$3.7x10^{-5}$	9.6	2.2	6.3
.4	$3.4x10^{-5}$	$1.3x10^{-4}$	2.6	8.5
.5	$4.2x10^{-5}$	1.6	3.0	$1.1x10^{-4}$
.6	$4.9x10^{-5}$	1.9	3.2	1.3

Dark Current — Run W-13, Temp. 25°C

$I_{F,R}$, a/cm^2

V/F	3*	5*	7*	8*
.01	1.6×10^{-6}	8.9×10^{-7}	8.5×10^{-6}	3.5×10^{-8}
.04	9.0	4.9×10^{-6}	3.4×10^{-5}	1.4×10^{-7}
.08	3.0×10^{-5}	1.6×10^{-5}	6.7	2.4
.10	4.7	2.6	8.4	3.1
.15	1.1×10^{-4}	6.8	1.3×10^{-4}	4.8
.20	2.1	1.4×10^{-4}	1.7	6.5
.25	3.5	2.4	2.3	9.0
.30	5.2	3.8	3.0	1.2×10^{-6}
.35	7.3	5.6	3.8	1.4
.40	1.0×10^{-3}	7.9	5.1	1.2
.45	1.4	1.1×10^{-3}	7.4	1.3
.50	2.3	1.9	1.3×10^{-3}	1.7
V/R				
.05	4.1×10^{-6}	2.7×10^{-6}	4.3×10^{-5}	3.9×10^{-7}
.1	5.7	4.3	8.7	8.1
.2	7.7	7.2	1.8×10^{-4}	1.5×10^{-6}
.3	9.2	1.0×10^{-5}	2.7	2.1
.4	1.0×10^{-5}	1.3	3.6	2.6
.5	1.1	1.6	4.6	3.1
.6	1.3	1.9	5.6	3.6

*Control cell

Table 8 W-4 28°C

Spectral Response, mA/mW-cm^2

Filter	1	2	3	4	5	6	7	8	9	10	11	12	13
λ	.45	.50	.55	.60	.65	.70	.75	.80	.85	.90	.95	.41	1.05
1	.282	.384	.466	.487	.517	.552	.594	.623	.634	.667	.589	.113	.207*
2	.300	.393	.469	.484	.512	.543	.587	.620	.632	.675	.606	.123	.216*
3	.289	.380	.451	.458	.477	.488	.507	.517	.498	.464	.378	.113	.116
4	.304	.386	.450	.453	.466	.467	.489	.506	.488	.456	.383	.123	.116
5	.284	.378	.455	.469	.494	.514	.543	.563	.554	.544	.452	.113	.142*
6	.294	.391	.468	.483	.512	.543	.587	.617	.632	.667	.598	.123	.221*
7													
8													
9	.279	.378	.463	.483	.514	.548	.590	.620	.632	.658	.576	.113	.195*
10	.299	.393	.469	.481	.511	.543	.579	.610	.630	.658	.606	.123	.216*
11	.284	.371	.441	.443	.460	.459	.478	.493	.480	.439	.366	.113	.105
12	.254	.347	.428	.441	.461	.454	.478	.506	.485	.430	.374	.098	.111
13	.294	.391	.468	.483	.507	.534	.576	.614	.622	.649	.589	.118	.216*
14	.274	.376	.460	.437	.513	.552	.587	.625	.632	.667	.598	.113	.211*

* Control cell

Table 9 W- 11 28°C

Spectral Response, mA/mW-cm^2

Filter	1	2	3	4	5	6	7	8	9	10	11	12	13
λ	.45	.50	.55	.60	.65	.70	.75	.80	.85	.90	.95	.41	1.05
1	.288	.394	.439	.461	.475	.481	.500	.507	.474	.429	.329	.127	.090
2	.297	.403	.447	.470	.484	.491	.514	.518	.492	.447	.351	.134	.102
3	.284	.396	.443	.470	.484	.489	.510	.514	.486	.437	.344	.124	.096
4	.284	.391	.435	.461	.477	.483	.512	.519	.490	.454	.354	.127	.098
5	.283	.387	.431	.449	.460	.452	.464	.468	.427	.362	.281	.121	.074
6	.278	.384	.435	.460	.478	.483	.500	.519	.480	.427	.331	.121	.092
7	.283	.393	.438	.463	.477	.479	.500	.507	.477	.427	.331	.121	.086
8	.283	.391	.442	.469	.490	.497	.523	.539	.514	.473	.382	.121	.110
9	.293	.399	.443	.468	.484	.492	.520	.527	.504	.464	.373	.127	.110
10													
11	.283	.393	.441	.465	.482	.488	.512	.524	.496	.454	.359	.127	.104
12	.283	.393	.439	.465	.480	.488	.508	.510	.483	.445	.345	.121	.104
13	.299	.395	.441	.464	.480	.479	.504	.507	.488	.445	.359	.127	.116
14	.283	.393	.439	.464	.478	.483	.508	.519	.496	.445	.354	.127	.098
15	.299	.397	.436	.458	.473	.489	.509	.511	.485	.445	.350	.138	.101
16	.294	.393	.431	.448	.456	.456	.466	.449	.422	.364	.275	.138	.073
17	.294	.388	.426	.443	.453	.447	.470	.471	.459	.409	.354	.138	.107
18	.299	.397	.419	.447	.454	.456	.466	.463	.433	.391	.297	.144	.090
19													
28	.294	.391	.433	.455	.467	.470	.490	.480	.461	.418	.328	.126	.101
21	.289	.393	.435	.456	.471	.479	.494	.491	.459	.409	.310	.132	.084
22	.289	.397	.440	.464	.477	.488	.505	.491	.469	.409	.319	.132	.090
23	.289	.393	.437	.463	.478	.493	.517	.523	.501	.464	.368	.132	.113
24	.294	.397	.440	.466	.478	.493	.505	.500	.474	.427	.332	.132	.096
25	.294	.393	.432	.451	.459	.461	.474	.469	.435	.373	.301	.132	.090
26	.294	.393	.433	.452	.462	.461	.478	.471	.448	.409	.314	.132	.096
27	.278	.384	.419	.441	.450	.452	.462	.457	.433	.373	.297	.126	.084

* Control cell

Table 3 W-11 continued

Spectral Response, $mA/mW-cm^2$

Filter	1	2	3	4	5	6	7	8	9	10	11	12	13
λ	.45	.50	.55	.60	.65	.70	.75	.80	.85	.90	.95	.41	1.05
1	.284	.394	.447	.480	.505	.533	.576	.594	.614	.627	.572	.132	.219*
2													
3	.278	.386	.436	.471	.495	.524	.568	.579	.603	.627	.554	.132	.214*
4	.284	.393	.444	.478	.504	.533	.580	.594	.619	.645	.585	.132	.231*
5	.289	.378	.441	.478	.502	.524	.560	.577	.587	.582	.505	.132	.180*
6	.284	.393	.444	.478	.502	.533	.576	.594	.614	.636	.563	.132	.214*
7	.273	.388	.440	.473	.500	.520	.564	.579	.598	.609	.541	.132	.191*
8	.284	.394	.444	.478	.501	.529	.576	.585	.616	.645	.590	.132	.231*

* Control cell

Table 10 W-12 28°C

Spectral Response, mA/mW-cm^2

Filter	1	2	3	4	5	6	7	8	9	10	11	12	13
λ	.45	.50	.55	.60	.65	.70	.75	.80	.85	.90	.95	.41	1.05
1	.231	.340	.402	.439	.470	.497	.541	.579	.586	.598	.538	.098	.186*
2													
3	.277	.386	.434	.463	.484	.506	.549	.582	.594	.604	.551	.126	.202*
4	.267	.365	.412	.439	.463	.488	.525	.552	.562	.569	.506	.119	.183*
5	.255	.357	.409	.443	.469	.497	.541	.573	.586	.603	.551	.114	.204*
6													
7													
8	.263	.374	.431	.464	.490	.516	.557	.582	.597	.611	.538	.113	.193*
9													
1-A	.228	.333	.389	.417	.437	.442	.453	.446	.420	.362	.264	.092	.068
1-D	.245	.350	.403	.430	.447	.456	.473	.455	.444	.385	.291	.100	.075
2	.262	.365	.407	.429	.439	.442	.457	.443	.423	.370	.278	.108	.077
3	.255	.363	.413	.433	.445	.442	.449	.437	.409	.340	.250	.102	.061
4	.251	.352	.402	.426	.441	.437	.461	.461	.463	.417	.358	.105	.111
5	.254	.361	.412	.436	.447	.437	.461	.455	.452	.392	.338	.104	.098
6	.247	.354	.410	.432	.447	.442	.461	.464	.457	.402	.344	.100	.099
7	.235	.344	.400	.433	.455	.465	.489	.485	.476	.437	.352	.098	.101
8	.224	.323	.381	.405	.423	.405	.426	.434	.433	.361	.318	.091	.086
9	.220	.331	.395	.433	.457	.469	.497	.491	.487	.438	.361	.088	.106
10	.251	.361	.415	.444	.463	.469	.489	.491	.476	.429	.352	.104	.103
11	.226	.333	.392	.426	.447	.456	.477	.467	.463	.421	.335	.092	.092
12	.227	.338	.402	.437	.461	.469	.497	.491	.487	.444	.357	.092	.100
13	.226	.338	.397	.430	.450	.456	.481	.464	.463	.416	.329	.091	.087
14	.220	.329	.390	.423	.447	.451	.473	.476	.463	.407	.334	.089	.090
15	.227	.338	.398	.430	.451	.460	.477	.467	.455	.404	.319	.093	.090

* Control Cell

Table 11 W-13 28°C

Spectral Response, mA/mW-cm^2

Filter	1	2	3	4	5	6	7	8	9	10	11	12	13
λ	.45	.50	.55	.60	.65	.70	.75	.80	.85	.90	.95	.41	1.05
1	.262	.374	.419	.441	.448	.453	.459	.446	.424	.384	.280	.107	.072 *
2	.253	.354	.391	.411	.420	.426	.441	.430	.417	.382	.299	.105	.076
3													
4	.279	.385	.421	.440	.445	.448	.457	.438	.423	.374	.288	.118	.075 *
5													
6	.269	.384	.430	.454	.464	.469	.481	.463	.452	.413	.320	.109	.071
7	.271	.381	.426	.453	.467	.474	.497	.491	.490	.451	.377	.112	.096
8	.268	.373	.416	.436	.447	.443	.461	.460	.455	.403	.352	.112	.088
9													
10													
11	.262	.377	.425	.451	.460	.469	.485	.463	.463	.441	.348	.106	.090
12	.270	.386	.438	.466	.480	.488	.513	.509	.511	.485	.411	.109	.106
13	.257	.381	.432	.463	.476	.483	.509	.506	.506	.473	.404	.106	.104
14	.263	.381	.434	.463	.479	.488	.509	.503	.503	.469	.386	.106	.097
15													
16	.254	.371	.423	.451	.463	.472	.485	.481	.461	.413	.330	.097	.078 *
17	.249	.366	.417	.447	.460	.469	.489	.478	.468	.431	.351	.099	.087
18	.275	.388	.434	.460	.471	.478	.501	.500	.492	.455	.383	.114	.100
19	.267	.386	.433	.460	.470	.479	.497	.488	.479	.435	.346	.112	.080
20													
21	.271	.379	.414	.433	.436	.437	.445	.424	.399	.345	.258	.116	.058
22	.282	.390	.426	.447	.466	.452	.461	.433	.425	.387	.293	.117	.068
23													
24	.263	.379	.424	.451	.460	.465	.481	.466	.452	.409	.322	.105	.075
25	.236	.343	.383	.407	.412	.416	.425	.402	.383	-	.254	.093	.060 *

* Corrected for area

Appendix Table 3 W-13 28°C

Spectral Response, $mA/mW\text{-}cm^2$

Filter	1	2	3	4	5	6	7	8	9	10	11	12	13
λ	.45	.50	.55	.60	.65	.70	.75	.80	.85	.90	.95	.41	1.05
1	.262	.386	.443	.480	.502	.530	.569	.588	.605	.623	.558	.109	.202 *
2	.222	.366	.431	.469	.489	.493	.537	.552	.575	.562	.516	.069	.155 *
3	.268	.390	.446	.484	.506	.534	.577	.594	.618	.643	.585	.113	.215 *
4	.261	.386	.445	.481	.505	.530	.573	.585	.610	.623	.567	.109	.173 *
5	.273	.388	.438	.471	.492	.516	.557	.570	.597	.624	.576	.115	.186 *
6	.274	.381	.426	.459	.479	.502	.545	.558	.580	.605	.544	.119	.170 *
7	.279	.390	.434	.466	.485	.506	.545	.561	.580	.597	.530	.117	.158 *
8	.286	.394	.439	.470	.490	.516	.553	.573	.599	.625	.581	.127	.183 *

* Control cell